JOURNAL OF GEOPHYSICAL RESEARCH, VOL. 104, NO. D23, PAGES 30,427-30,444, DECEMBER 20, 1999

Molecular hydrogen in the troposphere: Global distribution and budget

Paul C. Novelli, Patricia M. Lang, Kenneth A. Masarie,[1] Dale F. Hurst,[1]
Richard Myers,[2] and James W. Elkins

Climate Monitoring and Diagnostics Laboratory, National Oceanic and Atmospheric Administration, Boulder, Colorado

Abstract. Molecular hydrogen (H_2) has been measured since 1989 in air samples collected using a globally distributed sampling network. Time series from 50 locations are used to better define the distribution and recent changes of H_2 in the remote lower troposphere. These data show that the globally averaged H_2 mixing ratio between 1991 and 1996 was about 531 ± 6 parts per billion (ppb). Hydrogen exhibited well-defined seasonal cycles in each hemisphere, with similar seasonal maxima (530-550 ppb). However, in the Northern Hemisphere the seasonal minimum was 70 ppb deeper than in the Southern Hemisphere (~450 and 520 ppb, respectively), resulting in ~3% more H_2 in the south than in the north. With these data we have reevaluated the global H_2 budget. Methane oxidation is the largest source of H_2 to the troposphere, and soil uptake accounts for much of its sink. The global annual turnover is estimated as ~75 Tg H_2 yr^{-1}. The annual turnover, combined with a calculated tropospheric burden of 155 Tg, indicates a lifetime of ~2 years. While our understanding of the global distribution of the sources and sinks of H_2 is still incomplete, the lower annual minimum in the north may be reasonably attributed to hemispheric asymmetry in uptake by soils. The seasonal cycles in the two hemispheres show unusual similarities: the northern and the southern seasonal maxima and minima were offset by only a few months. We suggest that the seasonal cycle in the Southern Hemisphere is dominated by H_2 emissions from biomass burning.

1. Introduction

The relatively few measurements of atmospheric hydrogen (H_2) reported in the literature provide a variety of mixing ratios and global distributions. Schmidt and coworkers reported surface H_2 mixing ratios were ~540-590 ppb in the clean troposphere and ~800 ppb in an urban area [*Schmidt and Seiler* 1970; *Schmidt*, 1974; *Ehhalt et al.*, 1977]. This group also noted that background levels in the Northern Hemisphere (NH) were ~5% greater than in the Southern Hemisphere (SH). In contrast, *Khalil and Rasmussen* [1989, 1990] measured H_2 during 1986-1989 at six locations with latitudes ranging from 71°N to 90°S and found higher levels in the SH (~520 ppb) than in the NH (~490 ppb). The 3-year time series also showed an average annual increase of 0.6 ± 0.1% H_2 yr^{-1}.

Four main sources of H_2 to the troposphere have been identified [*Seiler and Conrad,* 1987; *Warneck*, 1988, and references therein]. These include two photochemical sources (the oxidation of methane (CH_4) and the oxidation of nonmethane hydrocarbons (NMHCs)) and two combustion sources (technological sources such as fossil fuel combustion, and biomass burning). These account for ~90% of the total source. The other 10% is attributed to emissions from volcanoes, the oceans, and production during nitrogen fixation by legumes. The biogeochemical cycle of H_2 is coupled to the atmospheric cycles of methane (CH_4) and carbon monoxide (CO) through the production and destruction of formaldehyde (HCHO).

Hydrogen is removed from the troposphere by reaction with OH [*Grenier*, 1969; *Schmidt*, 1974]:

$$H_2 + OH \rightarrow H_2O + H \quad (1)$$

and by deposition at the Earth's surface [*Schmidt*, 1974; *Conrad and Seiler*, 1980, 1985]. Soil deposition is biologically driven, possibly through the enzymatic activity of soil hydrogenases [*Conrad and Seiler*, 1980], and is typically the largest term in the global budget.

As part of the National Oceanic and Atmospheric Administration's Climate Monitoring and Diagnostics Laboratory (NOAA/CMDL) cooperative air sampling network, samples of air are collected from locations around the world and returned to our laboratory in Boulder for analysis of multiple trace gas species, including H_2, CO, CH_4, and carbon dioxide (CO_2) and its stable isotopes. Samples from all sites are analyzed with dedicated instruments and well-maintained reference scales, and they provide long-term, internally consistent time series of these compounds. These can then be used to constrain models of their biogeochemical cycles. In this paper we discuss the tropospheric distribution of hydrogen and its global budget.

2. Methods

2.1. Sample Collection

Hydrogen was measured in a subset of air samples collected using the NOAA/CMDL cooperative air sampling network

[1]Also at Cooperative Institute for Research in Environmental Sciences, University of Colorado, Boulder.

[2]Now at Standards and Certification Center, National Institute for Standards and Technology, Gaithersburg, Maryland.

Copyright 1999 by the American Geophysical Union.

Paper number 1999JD900788.
0148-0227/99/1999JD900788$09.00

(Figure 1). Sampling locations in this network represent the marine boundary layer (MBL), the regionally polluted boundary layer, and the free troposphere. Beginning in 1989, H_2 mixing ratios were determined at five sites. The number of locations was increased year by year until by the end of 1994, H_2 was measured at 52 sites around the world. Air samples were collected about once per week at 35 land sites, and approximately once every 3 weeks from a commercial container ship whose cruise track crossed the Pacific Ocean from North America to New Zealand. The 18 shipboard sampling locations were centered on 5° latitude bands between 45°N and 40°S. Owing to a paucity of samples from 45°N, 40°N, and 40°S, data from these sites were not included in the global analysis. Details of the site locations are given by *Conway et al.* [1994] and *Novelli et al.* [1998]. Samples were collected in 0.5-, 2.5-, or 3-L Pyrex flasks fitted with two glass piston stopcocks holding Teflon O-rings. The air was not dried during collection. One of two filling procedures was used: (1) a portable pumping system, which filled two flasks (volume of 0.5 or 2.5 L) in series to a pressure of ~1.3 atm; or (2) two 3-L flasks which had been previously evacuated in Boulder and then filled to atmospheric pressure on site. The two methods, compared by collocated sampling at three locations, gave similar results. The pumping system was typically used at land sites, and the evacuated flasks were used for shipboard sampling. One exception was Christmas Island, where air samples were collected using evacuated flasks. The stability of H_2 in flasks constructed of different materials (including stainless steel, aluminum, and glass) was examined in conjunction with tests for CO stability [*Novelli et al.*, 1992]. Results from these experiments indicated that H_2 mixing ratios were stable to within ~1% (at ~530 ppb) for 1 year in glass flasks. Samples were typically analyzed within a few months of sampling, except those from Antarctica, which may have had storage periods of up to a year. Two flask samples collected at nearly the same time are referred to as a flask pair. Flask designs, storage tests, and methods of sample collection were those used in the NOAA/CMDL CO and CH_4 programs [*Novelli et al.*, 1992, 1998; *Dlugokencky et al.*, 1994].

2.2. Analytical Methods

H_2 was measured using gas chromatography followed by hot mercuric oxide (HgO) reduction and UV absorption detection. This technique is based upon the reduction of solid HgO to mercury vapor by a reduced compound such as H_2 or CO. The resulting mercury vapor is then detected by UV absorption. From 1988 through November 1990, a reduction gas detector was used, and from December 1990 through 1996, samples were analyzed using a reduction gas analyzer. Both instruments were obtained from Trace Analytical, Inc. (Menlo Park, California), and were configured to measure H_2 and CO in air. Aliquots of the samples and standards were alternately passed through a cryogenic bath before flushing and filling the sample loop (volume of 2 mL). The air was then injected onto a

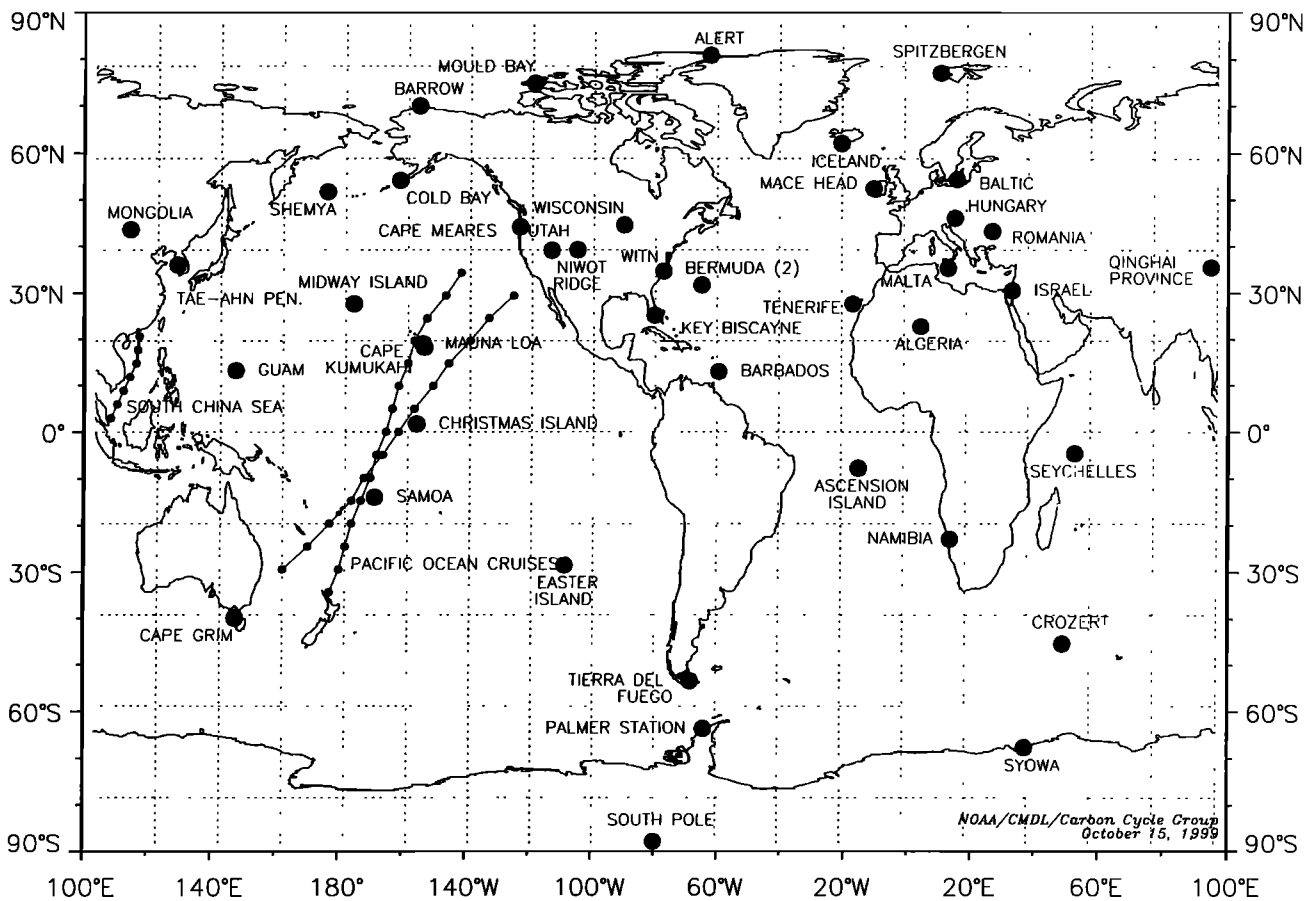

Figure 1. Map of sites from which air samples were analyzed for H_2: marine boundary layer (MBL) sites used in the global analysis (large solid circles), north and south ship tracks of the Pacific Ocean sampling program (small solid circles), and nonbackground or mountain top sites (triangles).

21562202d, 1999, D23, Downloaded from https://agupubs.onlinelibrary.wiley.com/doi/10.1029/1999JD900788 by INASP/HINARI - PAKISTAN, Wiley Online Library on [07/05/2025]. See the Terms and Conditions (https://onlinelibrary.wiley.com/terms-and-conditions) on Wiley Online Library for rules of use; OA articles are governed by the applicable Creative Commons License

chromatographic precolumn (Unibeads 1S) that was backflushed to remove CO_2, H_2O, and various hydrocarbons. H_2, CH_4, and CO were then separated by an analytical column (Molecular Sieve 5A) before being carried into the detector. The analysis of each air sample was bracketed by that of a reference gas. Peak areas and heights were determined by a Hewlett-Packard computing integrator (model 3393 or 3396), and all chromatographic data were stored for future quantification. H_2 mixing ratios were calculated from the ratio of the peak height of the sample to that of the standard, times the mixing ratio assigned to the standard in use at the time.

2.3. Reference Gases

The five working standards used during 1989-1996 for daily sample analysis were contained in 29-L aluminum high-pressure cylinders fitted with brass valves with tapered threads. These were filled at Niwot Ridge, Colorado (elevation of 3475 m above sea level (asl)), to a pressure of ~2000 pounds per square guage (psig) using an oilless pump (RIX SA6, Rix Industries, Oakland, California) and anhydrous magnesium perchlorate as the drying agent. These standards were assigned provisional H_2 mixing ratios relative to a natural air standard (~500 ppb H_2) purchased in 1984 from Biospherics, Portland, Oregon [*Dlugokencky et al.*, 1994]. These provided a set of intercalibrated reference gases for daily use (Table 1, working standards). They have been stable relative to each other within the precision of the measurements (~1%) during the past 5-10 years (Figure 2).

We recently prepared H_2-in-air standards using gravimetric methods. The procedure was similar to that used previously to prepare the CMDL CO gravimetric standards [*Novelli et al.*, 1991]. High-purity H_2 (99.999%, Scott Specialty Gases, Plumsteadville, Pennsylvania) was first diluted by gravimetric methods to produce four daughters, each containing ~250 ppm (10^{-6} mol mol^{-1}) H_2. Zero air (Scott Marrin, Inc., Riverside, California), passed through a stainless steel trap containing Hopcalite (Mine Safety Appliances, Pittsburgh, Pennsylvania) to remove trace H_2, was used as the diluent gas. Two standards with mixing ratios reflecting atmospheric levels were created from each of these daughters. These were then analyzed against one another and an H_2 standard obtained from Scott Specialty Gases, certified to 520 ppb (±2%). Of the eight atmospheric level standards prepared, three were not used in the reference scale because they were found to lie 3-4% above the calibration curve generated with the other five standards. This discrepancy was attributed to a leak found in the blending manifold after their preparation. The remaining five air mixtures, ranging from 485 to 603 ppb H_2, were used to define the reference scale (Table 1, gravimetric standards). Mixing ratios are reported as dry air mole fraction (1 ppb = 10^{-9} mol mol^{-1}).

H_2 calibration curves indicated the instrument response was linear to within 1% over the range of the standards. The working standards used between 1988 and 1995 were calibrated against the gravimetric standards in 1996 and were reassigned mole fractions according to the new scale. The gravimetric-based scale was ~6% greater than the working scale and ~18% greater than the standard from Scott Specialty Gases. H_2 mixing ratios assigned to air samples during 1989-1995 were recalculated from the archived sample and standard peak height responses using the gravimetric-based reference scale (Table 1).

2.4. Data Selection

The NOAA/CMDL cooperative air sampling program was developed to study the distribution of trace gases in the lower atmosphere, and sampling procedures were designed to collect air representing regional-scale air parcels free from local contamination. Unavoidably, samples were sometimes collected under nonbackground conditions. These samples were identified using the criteria described below, flagged in the data base, and omitted from the global analysis. The quality assurance procedure first identified analytical artifacts based upon chromatographic parameters (e.g., unacceptable baseline codes or retention times). Second, the agreement between two flasks of a pair was used to assess the quality of both the sampling and analytical procedures. If a flask mixing ratio minus the mean of the pair was greater than ±7.5 ppb H_2 (~1.5 times the analytical precision), both samples were flagged. Data passing the above

Table 1. H_2 Standards

CylinderID	Type of Cylinder[a]	Dates of Use[b]	H_2 Mixing Ratios		Rate of Change,[e] ppb yr^{-1}
			Working[c]	Grav[d]	
		Working Standards			
CC68734	SM	Jan. 1988 to Dec. 1990	527.5	560.4	-0.16 ± 1.9
CC73100	SM	Jan. 1988 to Dec. 1990	507.4	538.7	-0.19 ± 1.5
AAL-17269	AC	Jan. 1991 to May 1992	471.0	504.8	-0.03 ± 1.9
AAL-17270	AC	May 1992 to Dec.1994	483.0	524.8	1.08 ± 3.2
CC105871	AC	Dec.1994 to May 1997	505.7	538.2	0.27 ± 1.7
		Gravimetric Standards			
CC73198	SM	Feb. 1995	—	485.0	—
CC86013	SM	Feb. 1995	—	518.8	—
CA01310	SM	Feb. 1996	—	582.9	—
CC86208	SM	Feb. 1996	—	594.5	—
CC86259	SM	Feb. 1995	—	603.0	—

[a]Type of cylinder, SM, Scott Marrin, Inc.; AC, Scott Specialty Gases with Aculife treatment.

[b]Dates are the period of use for working standards, and preparation date for gravimetric standards.

[c]H_2 mixing ratio based upon a preliminary scale.

[d]For working standards, H_2 mixing ratio is based upon the gravimetric scale. For gravimetric standards, H_2 mixing ratio is based upon gravimetric preparation.

[e]Rate of H_2 change in the standards (slope of least squares linear fit of H_2 mixing ratio to storage time) and 1 standard error of the mean.

21562202d, 1999, D23, Downloaded from https://agupubs.onlinelibrary.wiley.com/doi/10.1029/1999JD900788 by INASP/HINARI - PAKISTAN, Wiley Online Library on [07/05/2025]. See the Terms and Conditions (https://onlinelibrary.wiley.com/terms-and-conditions) on Wiley Online Library for rules of use; OA articles are governed by the applicable Creative Commons License

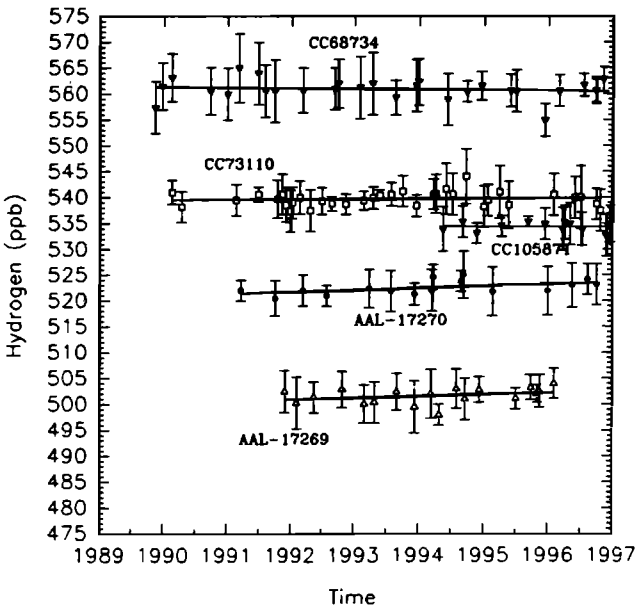

Figure 2. Histories of the working standards. Solid lines are the linear least squares regression fit to the data.

criteria were then fitted with a smooth curve [*Thoning et al.*, 1989]:

$$f(t) = a_1 + a_2 t + a_3 t^2 + \sum_{i=1}^{4} [a_{2i+1} \sin(2\pi i t) + a_{2i+2} \cos(2\pi i t)] \quad (2)$$

where t is time expressed in years and the coefficients a_i were determined from the curve fit. The curve-fitting procedure is based upon a least squares technique. Residuals from the curve were filtered using two low-pass filters (40 and 330 days), then added back to the function to yield the smooth curve. Outliers, those samples which deviated >3σ from the curve, were removed iteratively until no additional samples were flagged.

3. Time Series

Time series of H_2 mixing ratios from 50 locations (Figure 3) show the seasonal and latitudinal variations of this gas. Annually averaged H_2 mixing ratios in the boundary layer increased from the northern polar to tropical latitudes and reached a maximum in the southern tropics (Figure 4). Mixing ratios then decreased slightly in the high Southern Hemisphere (HSH). This gradient is largely driven by a seasonal drawdown that is stronger in the NH than in the south. While seasonal maximum H_2 mixing ratios were similar in both hemispheres (NH ≈ 530-550 ppb, SH ≈ 540-560 ppb) (Figures 3 and 5), the depth of the seasonal minimum varied considerably with latitude. In the high Northern Hemisphere (HNH), the seasonal minimum reached 420-440 ppb (Figure 5a), ~20% lower than the seasonal maximum, and in the northern tropics and extratropics, minimum mixing ratios ranged from 490 to 500 ppb, ~12% lower than the seasonal maximum. In the HSH the seasonal minimum ranged from 515 to 520 ppb (Figure 5b), just ~5-6% lower than the seasonal maximum. Mixing ratios in the tropics and subtropics exhibited greater short-term variability compared with those in the higher latitudes (Figure 3). These distributions primarily reflect differences in the location and timing of hydrogen sources and sinks in the two hemispheres.

We examined H_2 zonal distributions using a two-dimensional surface (H_2 versus latitude) in three-dimensional space (H_2 versus latitude versus time). Beginning June 1, 1990, weekly meridional curves were fit to the 39 individual time series from sites in the MBL (Figure 1) using the procedure described by *Tans et al.* [1989]. This created a series of latitudinal gradients from 90°N to 90°S. (In the higher latitudes where sites were lacking, mixing ratios were extrapolated from the nearest station to 90°; in the NH, Point Barrow (71°N) prior to 1992, then Alert (82°N); in the SH, Cape Grim (41°S) prior to 1993 and thereafter the South Pole.) A matrix of weekly mixing ratios averaged over 10° bands of latitude was extracted from these curves, which were combined and smoothed to create a latitudinal distribution of H_2 in the marine boundary layer. Zonally averaged time series representing the two hemispheres and the global average were extracted from the surface (Figure 6). These data also suggest a decline in H_2 during the course of the study.

The seasonal cycle of H_2 in the NH and the SH exhibited several differences. As noted above, the amplitude of the seasonal cycle in the NH was 3 times that in the SH. The relative timing of the seasonal maxima and minima were also different, with the maximum in the north occurring in late winter/early spring (March, April), while the SH the seasonal maximum occurred in late spring/early summer (December, January, February). In the LSH, greatest levels were found in September, October, November, ~3-4 months before the maximum in the HSH (January, February) (Figure 6). There were also differences in the timing of the seasonal minimums: in the NH, lowest H_2 mixing ratios were observed in late summer/early fall (August, September), while in the minimum in the SH occurred during late winter.

Combustion of fossil fuels and other industrial processes are considered to be significant sources of H_2 to the atmosphere (Table 2). However, we found that H_2 mixing ratios determined at polluted sites were not significantly greater than at those considered to represent clean air regions. For example, the time series determined at Mace Head, Ireland (MH, 53°20'N 9°54'W), represents clean air parcels arriving at the site from the North Atlantic. In contrast, samples collected over the Baltic Sea (BAL, 55°30'N 16°40'E) are thought to represent the regional signature of the polluted northern European boundary layer. Although the Baltic time series exhibits slightly greater mixing ratios and more variability compared with that for Mace Head, the two time series show similar features (Figure 7). On occasion, H_2 mixing ratios at BAL were 5-10% greater than those at MH (presumably as a result of sampling air that was transported to BAL from polluted continental Europe). In contrast, mixing ratios of CO (which has similar anthropogenic sources as H_2) are often 2 to 3 times greater at BAL than at MH [*Novelli et al.*, 1998].

4. Hydrogen Budget

The global H_2 budget is thought to consist of four major sources: two combustion sources, combustion from technological processes and the combustion of biomass, and two photochemical sources, the oxidation of CH_4 and the NMHCs. Two main sinks are recognized: reaction with OH and uptake by soils (Table 2). Here we reexamine H_2 source and sink strengths based upon recent insight into reaction pathways and estimates of precursor

21562202d, 1999, D23, Downloaded from https://agupubs.onlinelibrary.wiley.com/doi/10.1029/1999JD900788 by INASP/HINARI - PAKISTAN, Wiley Online Library on [07/05/2025]. See the Terms and Conditions (https://onlinelibrary.wiley.com/terms-and-conditions) on Wiley Online Library for rules of use; OA articles are governed by the applicable Creative Commons License

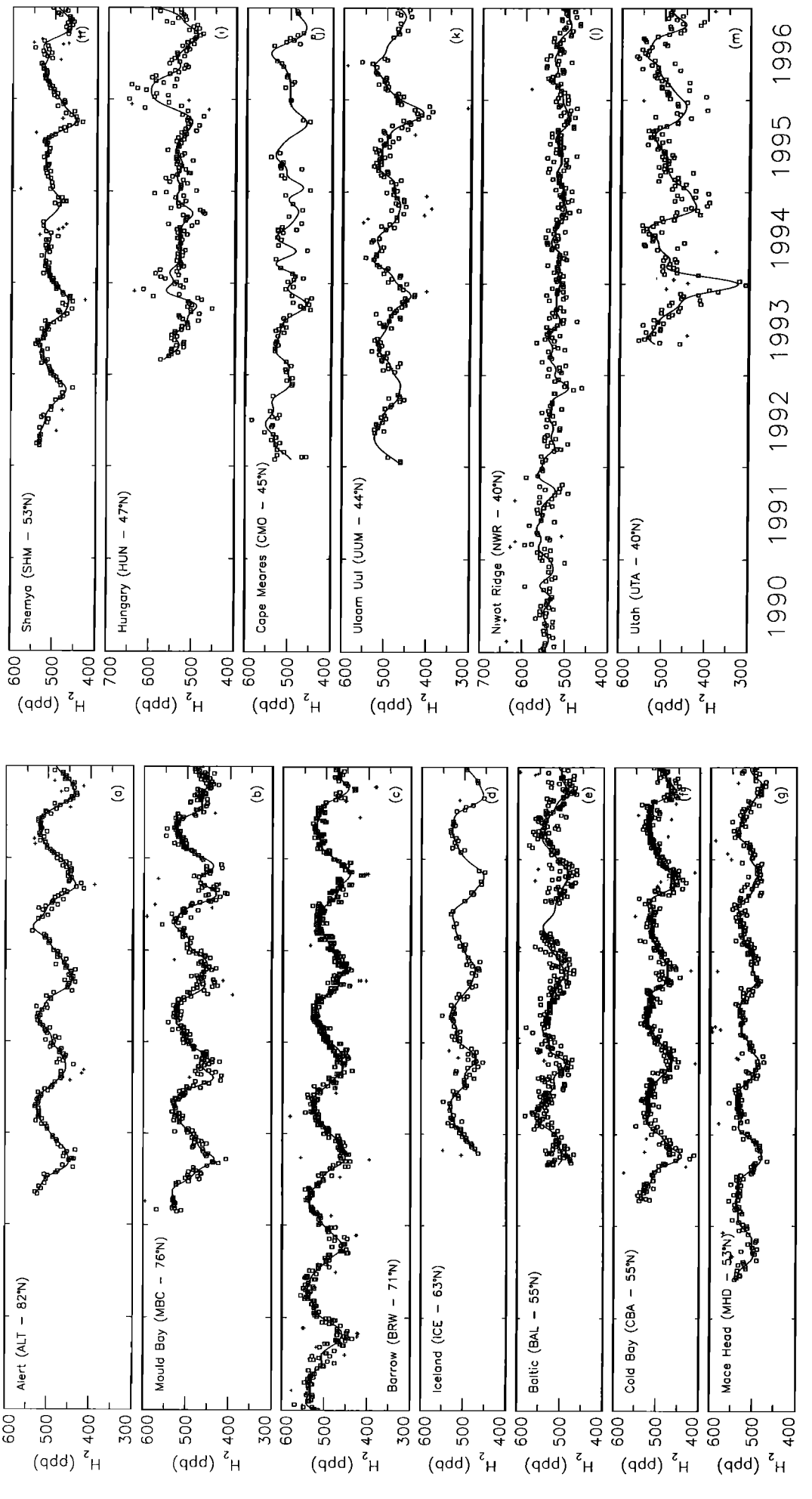

Figure 3. Hydrogen time series for sampling sites in the NOAA/CMDL cooperative air sampling network. The retained measured values (squares), rejected values (pluses), and the smoothed fit to the data are plotted.

21562202d, 1999, D23, Downloaded from https://agupubs.onlinelibrary.wiley.com/doi/10.1029/1999JD900788 by INASP/HINARI - PAKISTAN, Wiley Online Library on [07/05/2025]. See the Terms and Conditions (https://onlinelibrary.wiley.com/terms-and-conditions) on Wiley Online Library for rules of use; OA articles are governed by the applicable Creative Commons License

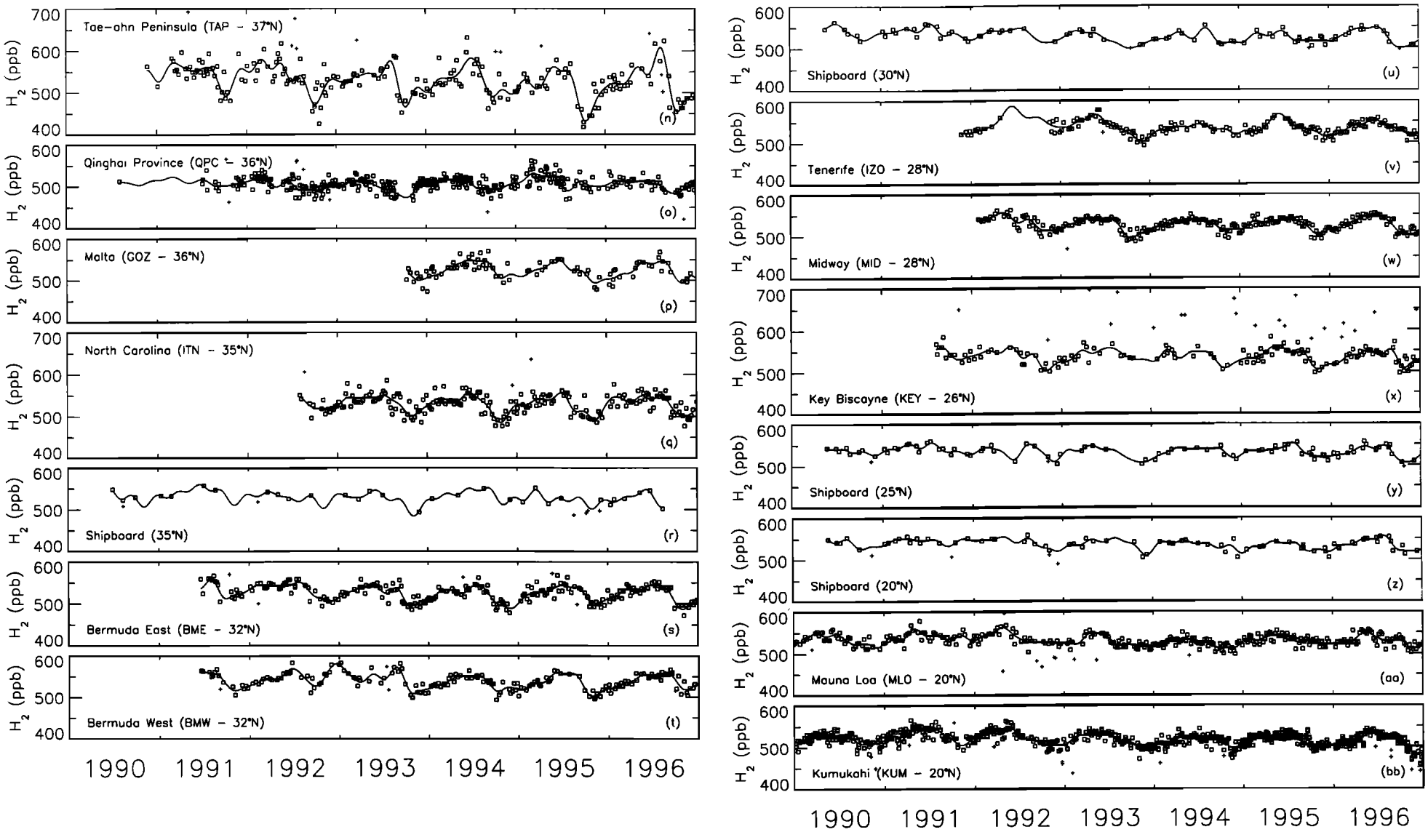

Figure 3. (continued)

21562024, 1999, D23, Downloaded from https://agupubs.onlinelibrary.wiley.com/doi/10.1029/1999JD900788 by INASP/HINARI - PAKISTAN, Wiley Online Library on [07/05/2025]. See the Terms and Conditions (https://onlinelibrary.wiley.com/terms-and-conditions) on Wiley Online Library for rules of use; OA articles are governed by the applicable Creative Commons License

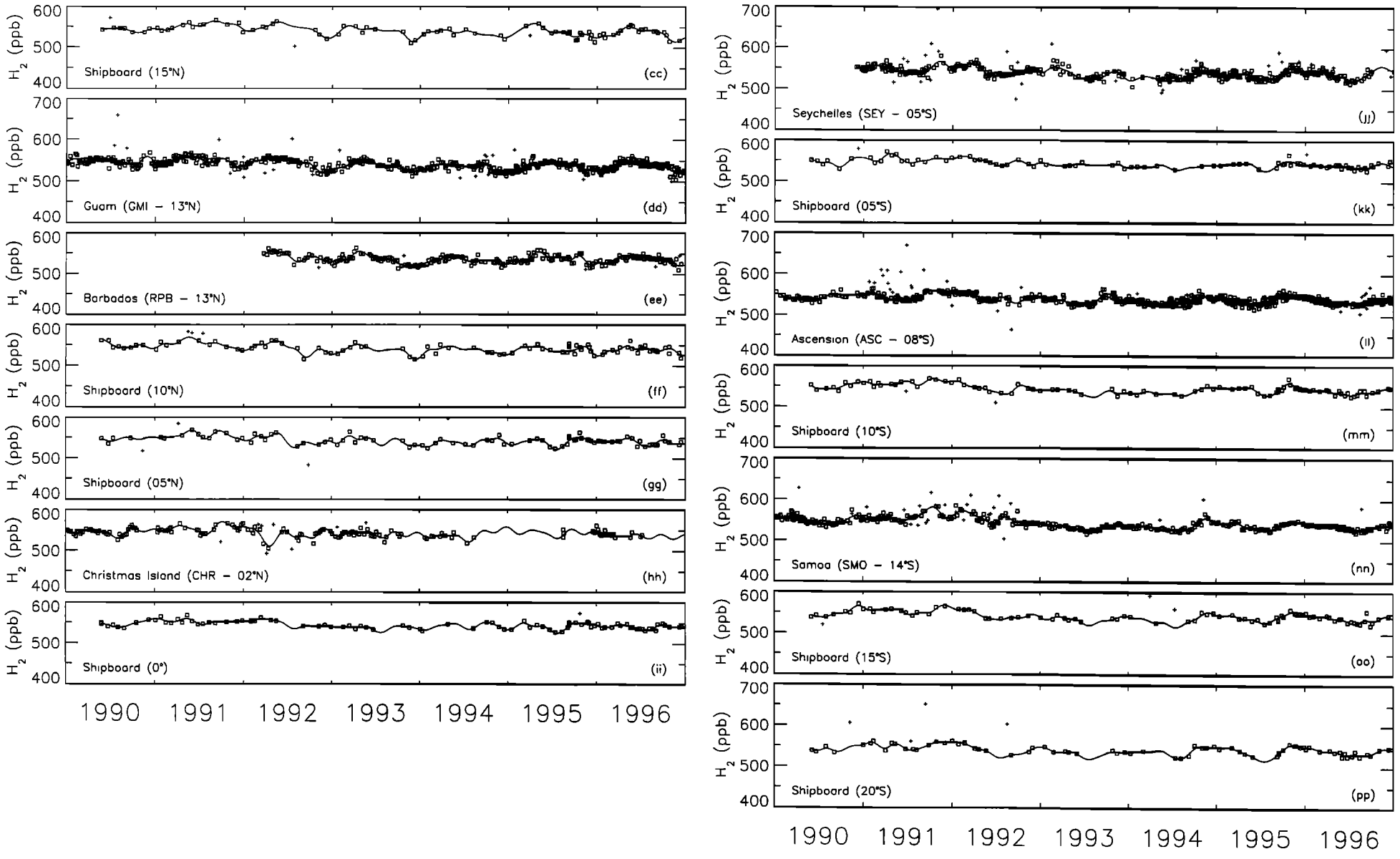

Figure 3. (continued)

21562202d, 1999, D23, Downloaded from https://agupubs.onlinelibrary.wiley.com/doi/10.1029/1999JD900788 by INASP/HINARI - PAKISTAN, Wiley Online Library on [07/05/2025]. See the Terms and Conditions (https://onlinelibrary.wiley.com/terms-and-conditions) on Wiley Online Library for rules of use; OA articles are governed by the applicable Creative Commons License

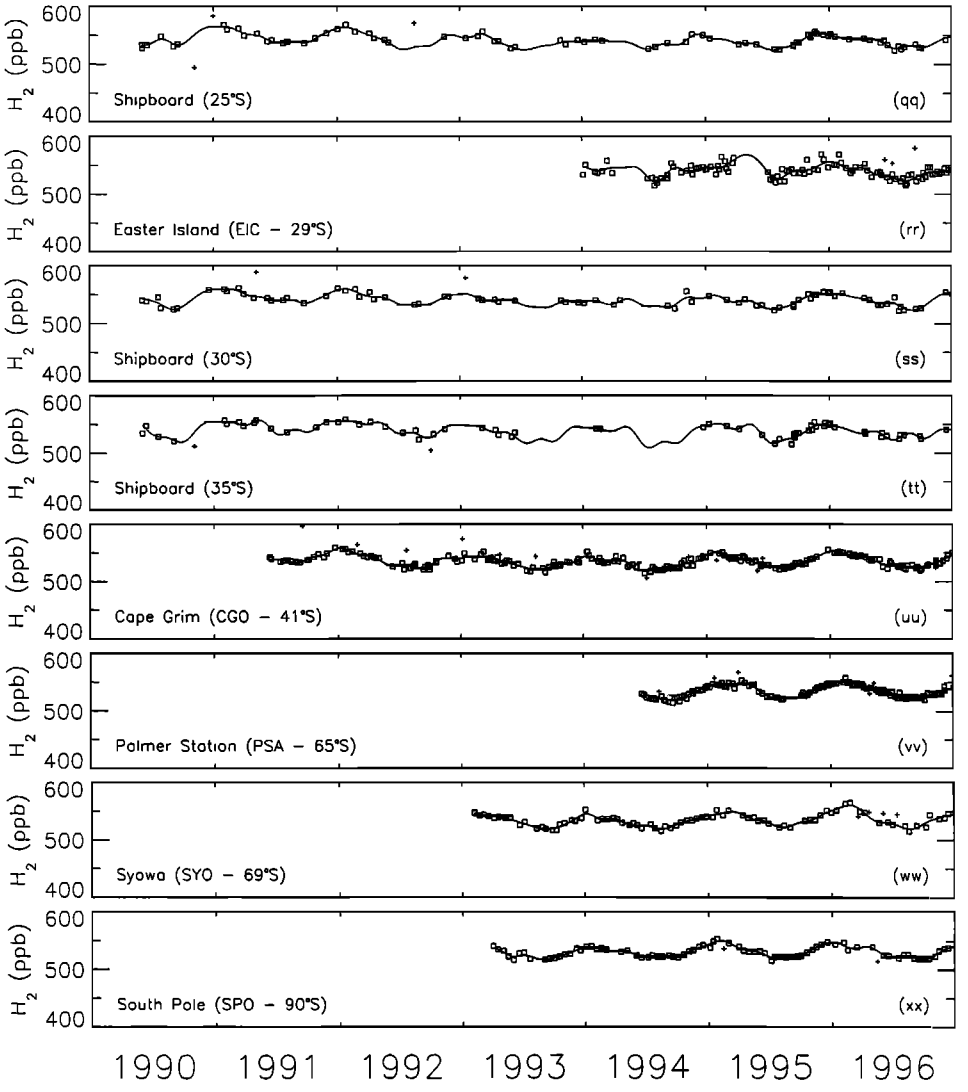

Figure 3. (continued)

emissions. The mean values for each source and sink determined below are provided in Table 2.

4.1. Hydrogen Sources

4.1.1. Photochemical sources. Hydrogen production from the oxidation of NMHCs is the result of reactions between a considerable number of compounds, with the reaction and photolysis rates for important chemical pathways dependent upon numerous, highly variable parameters. Here we focus on three key processes that drive H_2 production from hydrocarbons, (1) the production of formaldehyde during the oxidation of CH_4 and NMHCs; (2) the relative importance of HCHO loss by photolysis versus reaction with OH; and (3) the H_2 quantum yield from HCHO photolysis as a function of wavelength, temperature, and pressure (Figure 8).

The hydroxyl radical, the dominant oxidant in the troposphere, is produced following the photolysis of ozone:

$$O_3 + h\nu\ (\lambda < 315\ \text{nm}) \rightarrow O(^1D) + O_2 \quad (3)$$

$$O(^1D) + H_2O \rightarrow 2\ OH. \quad (4)$$

The oxidation of CH_4, initiated by reaction with OH (reaction (5)), proceeds through the formation of HCHO to CO (illustrated by the reaction sequence (5)-(12)). (Note that not all intermediates and less competitive reactions are shown; for a more complete review of the methane oxidation cycle see *Calvert* [1980] and *Ravishankara* [1988].):

$$CH_4 + OH \rightarrow CH_3 + H_2O \quad (5)$$

$$CH_3 + O_2 + M \rightarrow CH_3O_2 + M \quad (6)$$

$$CH_3O_2 + CH_3O_2 \rightarrow 2\ CH_3O + O_2 \quad (7a)$$

$$CH_3O_2 + HO_2 \rightarrow CH_3OOH + O_2 \quad (7b)$$

$$CH_3O_2 + NO \rightarrow CH_3O + NO_2 \quad (7c)$$

$$CH_3O_2 + CH_3O_2 \rightarrow CH_3OH + HCHO + O_2 \quad (7d)$$

$$CH_3OOH + h\nu \rightarrow CH_3O + OH \quad (8a)$$

$$CH_3OOH + OH \rightarrow CH_3O_2 + H_2O \quad (8b)$$

21562202d, 1999, D23, Downloaded from https://agupubs.onlinelibrary.wiley.com/doi/10.1029/1999JD900788 by INASP/HINARI - PAKISTAN, Wiley Online Library on [07/05/2025]. See the Terms and Conditions (https://onlinelibrary.wiley.com/terms-and-conditions) on Wiley Online Library for rules of use; OA articles are governed by the applicable Creative Commons License

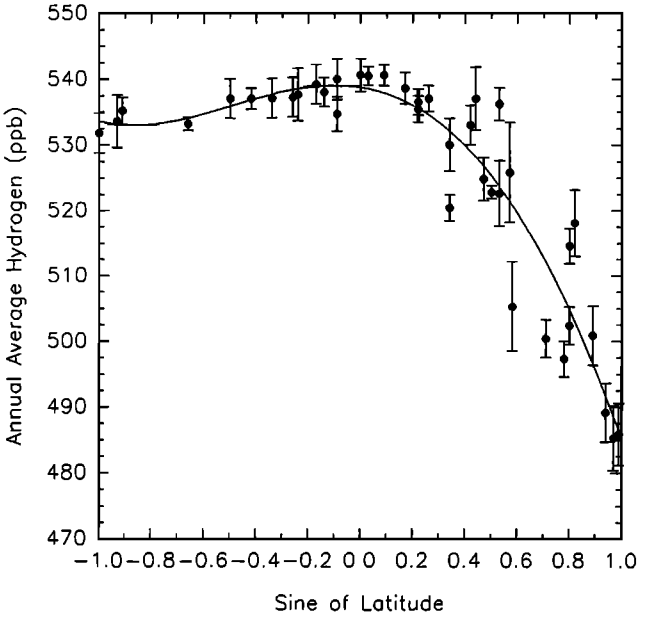

Figure 4. Annually averaged latitudinal gradient during 1992-1995. Error bars represent the standard deviation of the four annual means.

$$CH_3OOH + OH \rightarrow \rightarrow HCHO + H_2O + OH \quad (8c)$$

$$CH_3OH + OH + O_2 \rightarrow HCHO + HO_2 + H_2O \quad (9)$$

$$CH_3O + O_2 \rightarrow HCHO + HO_2 \quad (10)$$

$$HCHO + h\nu \rightarrow H + HCO \quad (11a)$$

$$\rightarrow H_2 + CO \quad (11b)$$

$$HCHO + OH \rightarrow \rightarrow CO \text{ and products.} \quad (12)$$

In regions of low NO_x ($NO + NO_2$) the primary route of HCHO formation from CH_4 oxidation is through reactions (5), (6), (7a), (7b), (8a), (8b), and (10). Production through (7c), (7d),(8c), and (9) is small [*Calvert,* 1980]. Wet deposition of stable reaction cycle intermediates, such as CH_3OOH, which would present a sink for carbon, are considered negligible [*Cohan et al.*, 1999]. In regions of sufficient NO_x (where [NO] is more than 10 times $[HO_2]$) the methylperoxy radical (CH_3O_2) formed by (6) reacts with NO to form CH_3O (reaction (7c)); which upon reaction with O_2 produces HCHO (reaction (10)). Here we assume that all CH_4 oxidized by OH ultimately yields formaldehyde.

Formaldehyde, which has a photochemical lifetime of the order of hours, either undergoes photolysis to produce H_2 and CO (reaction (11b)) or reacts with OH (reaction (12)) producing CO but no H_2 *(Calvert* [1980], *Ravishankara* [1988], and Figure 8). Nighttime reactions of O_3 and NO_3 with HCHO are assumed to produce little H_2 [*Stockwell and Calvert,* 1983]. We also assume that loss of HCHO through wet deposition is small (≤1%) compared to photochemical destruction [*Zafiriou et al.,* 1980; *Lowe and Schmidt,* 1983]. Several other studies of HCHO cycling also state that loss through wet deposition must be small (*Warneck et al.* [1978] (as referenced by *Lowe and Schmidt* [1983], *de Serves* [1994], and *Ayers et al.* [1997]), although these do not give a quantative estimate of the loss rate. Dry deposition also provides a small but somewhat more significant sink. We estimated the rate of HCHO loss by dry deposition (~15 Tg C from HCHO yr^{-1}) based upon surface deposition velocities of 0.3-0.8 cm s^{-1} [*Brasseur et al.*, 1998], tropospheric concentrations of HCHO between 0.3 ppb (background) and 2 ppb (urban) [*Graedel et al.*, 1976; *Lowe and Schmidt,* 1983; *de Serves,* 1994; *Solberg et al.*, 1996; *Ayers et al.*, 1997], and the surface regime areas from *Graedel and Crutzen* [1993]. If, as discussed above, all CH_4 oxidized produces HCHO, then the rate of HCHO production is equal to the rate of CH_4 destruction (~300 Tg C yr^{-1} [*Crutzen,* 1991]), and we find ~5% of HCHO formed may be lost through dry deposition.

The relative importance of each of the two photochemical loss pathways of HCHO (reactions (11) and (12)) depends upon both its cross section and the photon flux as a function of wavelength and on the HCHO and OH concentrations. These parameters are highly variable in space and time; hence rates of HCHO loss will have correspondingly high variation. Nonetheless, average HCHO destruction rates through reactions (11) and (12) are expected to be of similar magnitude [*Ravishankara,* 1988; *Fehsenfeld et al.*, 1992]. Comparison of photolysis rates and the HCHO + OH reaction rates (Table 3) suggests that the fraction of HCHO undergoing photolysis is somewhat greater than that oxidized by OH; however, we note that the rates presented in Table 3 contain considerable uncertainties.

Following the above discussion, the production rate of H_2 from CH_4 oxidation (P_{CH4}) can be estimated:

$$P_{CH4} = k_5\,[OH](G_{CH4})(0.95)(F_{HCHO})(\phi_2)(M), \quad (13)$$

where k_5 is the reaction rate constant of CH_4 + OH at an average tropospheric temperature of 277 K, $(4.0 \pm 0.2) \times 10^{-15}$ cm^3 $molecule^{-1}$ s^{-1}; [OH] is the average tropospheric OH concentration, $(9.7 \pm 0.6) \times 10^5$ molecules cm^{-3} [*Prinn et al.*, 1995]; and the total tropospheric burden of CH_4 (G_{CH4}) is ~4000 ± 400 Tg (0.82 × the atmospheric burden (4850) [*Intergovernmental Panel on Climate Change* (*IPCC*), 1996] (1 Tg = 10^{12} g). The factor 0.95 accounts for a 5% loss of HCHO to dry deposition. Although the fraction of HCHO photolyzed in the troposphere (F_{HCHO}) is highly variable, from Table 3 we estimate $F_{HCHO} \cong 0.65 \pm 0.15$. The mean yield of H_2 from reaction (11b) over the range of tropospheric conditions ($\phi_2 = 0.6 \pm 0.1$) was calculated for λ = 310-350 nm, temperature of 280 K, and pressure of ≈500 mbar using data from *Moortgat and Warneck* [1979] and *Moortgat et al.* [1983]. These values are similar to those reported by *Calvert.* [1980]. Last, M is the mass ratio of H_2/CH_4. The tropospheric source of H_2 from CH_4 oxidation is then determined to be between 12 and 40 Tg yr^{-1}. The uncertainty of the mean was computed as the error of each term in (13) propagated in quadrature [*Snedecor and Cochran,* 1967]. We estimate 26 ± 9 Tg H_2 yr^{-1} are produced from the oxidation of methane.

The oxidation of naturally occurring reactive nonmethane hydrocarbons (nNMHCs) via reaction with OH and other oxidants is a potentially large source of H_2 to the troposphere. As is the case for CH_4 oxidation, H_2 production from nNMHCs proceeds through HCHO. During the daytime, reaction with OH is the predominant oxidation pathway for most NMHCs, whereas at night, reaction with NO_3 becomes relatively more important. In the following discussion we assume that the oxidation products derived from the reaction of a hydrocarbon containing at

21562024, 1999, D23, Downloaded from https://agupubs.onlinelibrary.wiley.com/doi/10.1029/1999JD900788 by INASP/HINARI - PAKISTAN, Wiley Online Library on [07/05/2025]. See the Terms and Conditions (https://onlinelibrary.wiley.com/terms-and-conditions) on Wiley Online Library for rules of use; OA articles are governed by the applicable Creative Commons License

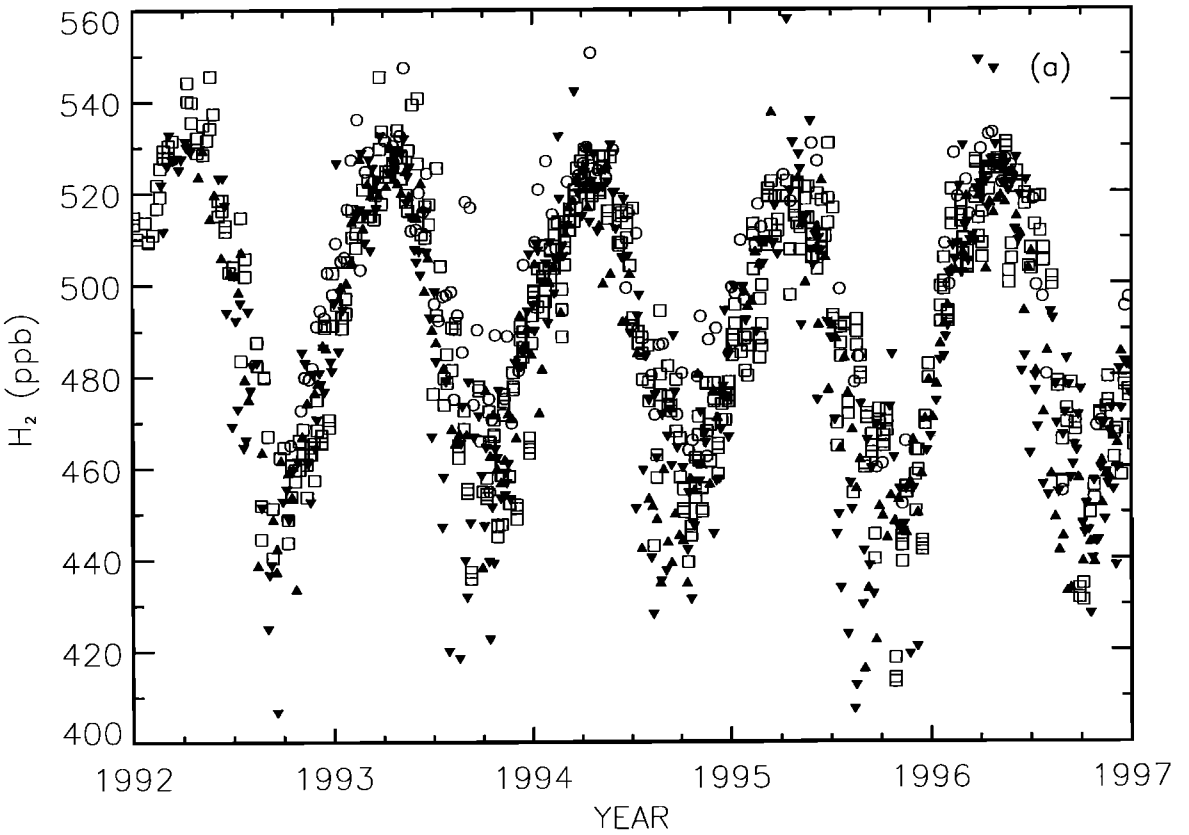

Figure 5a. H_2 time series at sites in the HNH, Iceland (63°N; circles), Point Barrow (71°N; squares), Mould Bay (76°N, inverted triangles), and Alert (82°N, triangles).

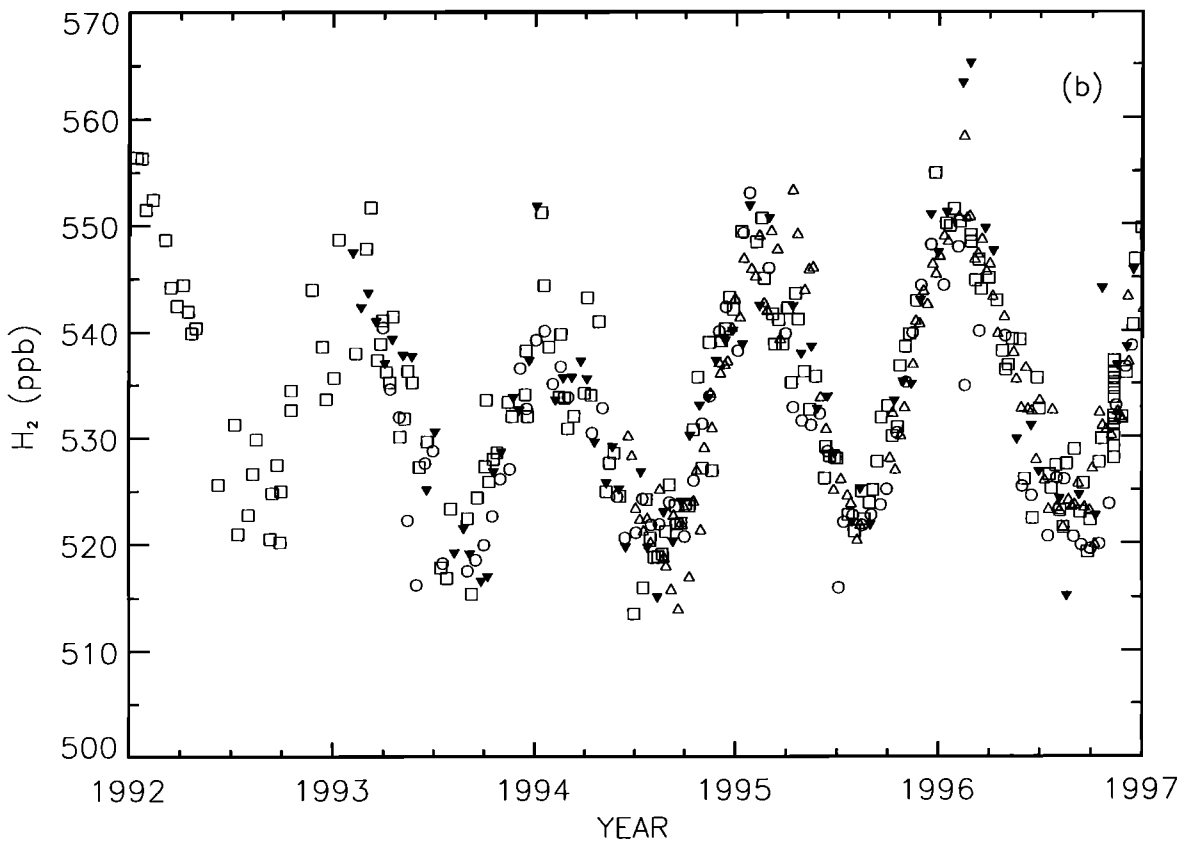

Figure 5b. H_2 time series at sites in the HSH, Cape Grim (41°S, squares), Palmer Station (63°S, trianges), Syowa (69°S, inverted triangle), and South Pole (circles).

21562202d, 1999, D23, Downloaded from https://agupubs.onlinelibrary.wiley.com/doi/10.1029/1999JD900788 by INASP/HINARI - PAKISTAN, Wiley Online Library on [07/05/2025]. See the Terms and Conditions (https://onlinelibrary.wiley.com/terms-and-conditions) on Wiley Online Library for rules of use; OA articles are governed by the applicable Creative Commons License

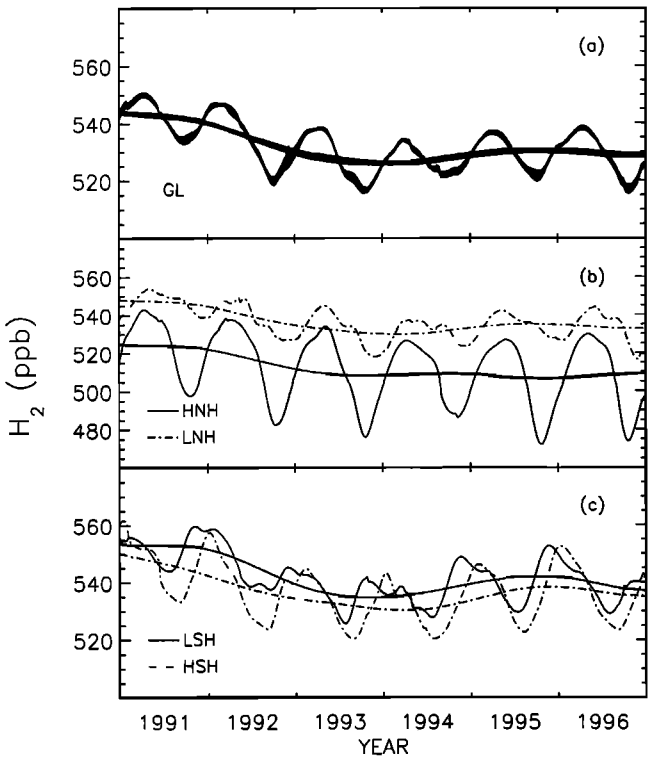

Figure 6. Zonally averaged time series and trends for 1991-1996. (a) Global average. Shaded areas around the smoothed curve represent the uncertainty of the global average mixing ratios and trends as determined using equation (2) with $a_3 = 0$ and a statistical bootstrap technique to estimate the uncertainty [*Steele et al.*, 1992]. (b, c) Zonal mean mixing ratios and trends for the four semihemispheres.

least one reactive C = C bond (e.g., isoprene) + NO_3 are similar to those derived from reaction with OH [*Fehsenfeld et al.*, 1992]. During the oxidation of CH_4, carbon is quantitatively oxidized to HCHO. In contrast, fractional yields of HCHO are common during nNMHC oxidation due to the high solubilities and very low vapor pressures of reaction cycle intermediates.

We used the Global Emissions Inventory Activity (GEIA) natural volatile organic carbon emission data set [*Guenther et al.*, 1995] to estimate the global rate of H_2 production from biogenic NMHCs (P_{NMHC}). P_{NMHC} was determined as the sum of the H_2 yields from the categories of natural hydrocarbons presented in the GEIA inventory: isoprene (C_5H_8); monoterpenes (e.g., $C_{10}H_x$); reactive nNMHCs that have lifetimes <1 day (including olefinic and aromatic alcohols), and other nNMHCs with lifetimes >1 day (including the aliphatic alcohols):

$$P_{NMHC} = \Sigma [(S_i Y_i)(0.95) F_{HCHO}(\phi_2) N_i)], \quad (14)$$

where S_i is the global source of nNMHC in category i (in Tg C yr^{-1}), and Y_i is the HCHO yield per carbon of $NMHC_i$. Five percent of the HCHO produced is lost through dry deposition. F_{HCHO}, as defined above, is the fraction of HCHO that undergoes photolysis to produce H_2 (= 0.65 ± 0.15). The branching ratio (ϕ_2) of reaction (11b) at the surface is 0.5 ± 0.1 [*DeMore et al.*, 1997]. N_i is the mass ratio of $H_2/(nNMHC_i$/[number of C in $nNMHC_i$]).

With a global source between 200 and 500 Tg C yr^{-1}, isoprene (C_5H_8) is the most abundant nNMHC emitted from plants to the troposphere [*Müller*, 1992; *Guenther et al.*, 1995]. Although details of its atmospheric cycle are still uncertain, the main products of C_5H_8 oxidation are known with some confidence. It is also clear that the reaction pathways and the products formed are dependent upon NO_x concentrations [e.g., *Fehsenfeld et al.*, 1992]. In regions of high NO_x, such as urban or regionally polluted continental areas and some forest environments, up to three molecules of HCHO may be produced per C_5H_8 molecule [*Jacob and Wofsy*, 1988; *Paulson and Seinfeld*, 1992]. In areas of low NO_x the yield of HCHO per isoprene may be much lower [*Jacob and Wofsy*, 1990; *Hatakeyama et al.*, 1991; D. Jacob, personal communication, 1998]. Assuming that between one and three molecules of HCHO are produced per molecule of C_5H_8 (Y_{C5H8} is between 0.2 and 0.6), the global source of H_2 from isoprene oxidation determined from (14) is 1-22 Tg H_2 yr^{-1}. Furthermore, C_5H_8 emissions largely occur in tropical forests, where photochemical and physical conditions favor low HCHO yields. Assuming 80%

Table 2. Global Budget of H_2 in the Troposphere

	Seiler and Conrad [1987]	*Warneck* [1988]	This Work[a]
		Sources	
Technological processes	20 ± 10	17	15 ± 10
Biomass burning	20 ± 10	15	16 ± 5
Methane oxidation	15 ± 5	29	26 ± 9
NMHC oxidation	25 ± 10	21	14 ± 7[b]
Biogenic N_2 fixation	3 ± 2	3	3 ± 1[c]
Oceans	4 ± 2	4	3 ± 2[d]
Total sources	87 ± 38	89	77 ± 16
		Sinks	
Oxidation by OH	8 ± 3	11	19 ± 5
Uptake by soils	90 ± 20	78	56 ± 41
Total sinks	98 ± 23	89	75 ± 41

Units are Tg H_2 yr^{-1}.

[a]The value for each individual source/sink term is the mean of the maximum and minimum estimate; the uncertainty is the propagated error of each term in the calculation. The total source/sink is the mean and propagated error of the individual sources/sinks.

[b]Calculated with the source of H_2 from C_5H_8 = 2-7 Tg yr^{-1} (see text for details).

[c]From *Conrad and Seiler* [1980].

[d]Following *Schmidt* [1974], using a thin film thickness of 25-75 μm.

215622024, 1999, D23, Downloaded from https://agupubs.onlinelibrary.wiley.com/doi/10.1029/1999JD900788 by INASP/HINARI - PAKISTAN, Wiley Online Library on [07/05/2025]. See the Terms and Conditions (https://onlinelibrary.wiley.com/terms-and-conditions) on Wiley Online Library for rules of use; OA articles are governed by the applicable Creative Commons License

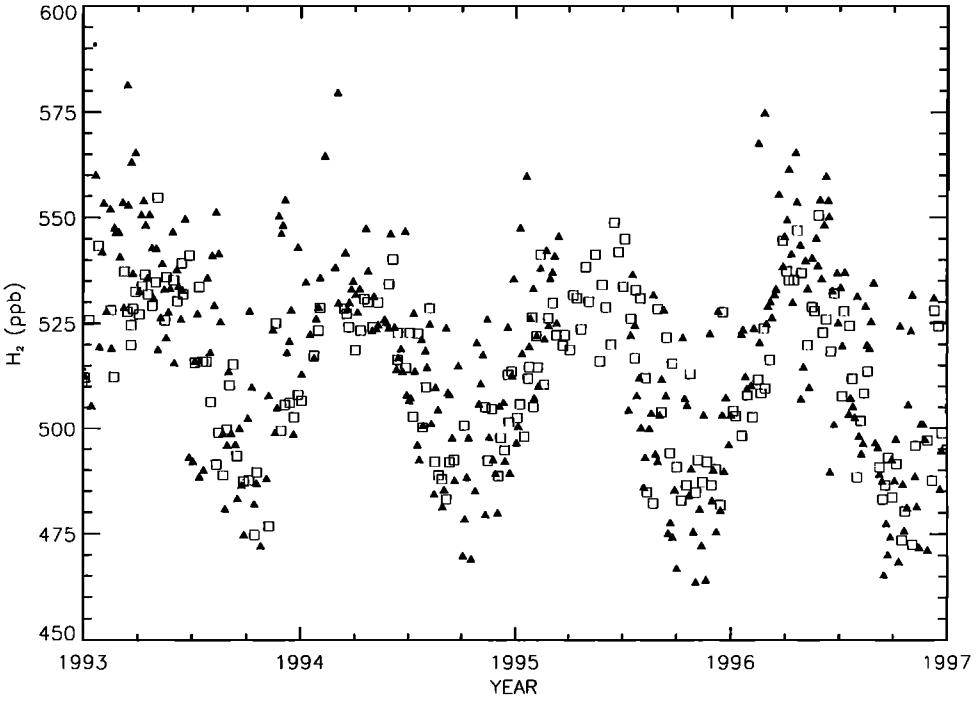

Figure 7. Time series of H_2 mixing ratios determined at Mace Head, Ireland (squares), and over the Baltic Sea (triangles).

of C_5H_8 oxidation occurs in areas of low NO_x [*Müller*, 1992] and 20% occurs in regions where NO_x is sufficiently high to force the C_5H_8 oxidation pathway to produce 3 HCHO, then considerably less H_2 production from isoprene oxidation (2-7 Tg yr^{-1}) is predicted.

Global emission rates of the monoterpenes have been estimated at 130 to 480 Tg C yr^{-1}; however, the more recent studies suggest rates near 150 Tg C yr^{-1} [*Zimmerman et al.*, 1978; *Taylor et al.*, 1990; *Müller*, 1992; *Guenther et al.*, 1995]. The oxidation of these alkenes is expected to result in a loss of reactive carbon through the production of aerosols [*Graedel*, 1979; *Hatakeyama et al.*, 1991]. Following *Müller and Brasseur* [1995], we assume that the HCHO yield from terpenes is 2 times lower than that from isoprene. This is consistent with the estimated yield of CO from the oxidation of terpenes (0.15) as suggested by *Hatakeyama et al.* [1991]. From (14), using a source strength of monoterpenes ranging from 100 to 200 Tg C yr^{-1}, these compounds provide 0.2-5 Tg H_2 yr^{-1} to the troposphere.

Biogenic NMHCs other than isoprene and the monoterpenes are ubiquitous in the troposphere; however, their distributions, emissions rates, and degradation pathways are poorly defined.

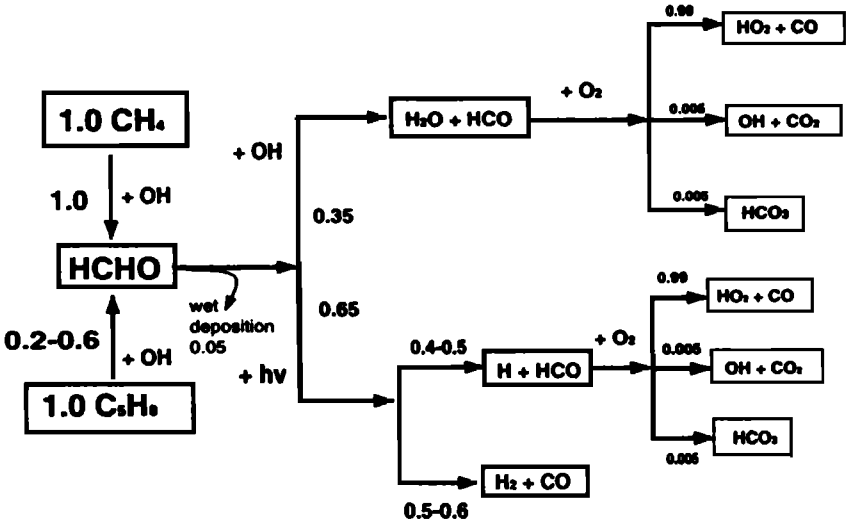

Figure 8. Schematic of the reaction pathways and yields used to calculate H_2 production during the oxidation of CH_4 and C_5H_8: molecules in boxes are the reaction products; fractions along the reaction pathways are the product yields.

21562024, 1999, D23, Downloaded from https://agupubs.onlinelibrary.wiley.com/doi/10.1029/1999JD900788 by INASP/HINARI - PAKISTAN, Wiley Online Library on [07/05/2025]. See the Terms and Conditions (https://onlinelibrary.wiley.com/terms-and-conditions) on Wiley Online Library for rules of use; OA articles are governed by the applicable Creative Commons License

Table 3. Ratio of HCHO Loss Rates By Photolysis to That by Reaction With OH for Clear-Sky Conditions, Noon January 1 and July 1 at 1000 and 500 mbar

	January		July	
Latitude	1000 mbar	500 mbar	1000 mbar	500 mbar
40°N	0.78/0.2	0.09/0.048	5.4/2.9	0.64/0.33
20°N	0.93/1.4	0 22/0.16	3.9/3.2	0.59/0.33
20°S	3.9/2.7	0.59/0.37	0.93/1.5	0.22/0.20
40°S	5.3/1.5	0.64/0.20	0 78/0.24	0 09/0.05

* Values, in units of 10^5 molecule cm^{-1} s^{-1}, are the ratio of the photolysis rate to the reaction rate determined for clear sky conditions noon January 1 and noon July 1 at 1000 and 500 mbar. Photolysis rate constants (k_p) were determined as $\sum \sigma(\lambda)\Theta(\lambda)J(\lambda)$, where $\sigma(\lambda)$ is the absorption cross section over λ = 290-360, $\Theta(\lambda)$ = wavelength-dependent quantum yield of reactions (1a)+ (1b), and $J(\lambda)$ is the noontime actinic flux under clear-sky conditions. Surface values for these parameters were obtained from *Demerjian et al* [1980] as provided by *Finlayson-Pitts and Pitts* [1986]. Actinic flux at 500 mbar was assumed to be 20% greater than the surface value (E. Dutton, personal communication, 1998), and $\sigma(\lambda)$ and $\Theta(\lambda)$ at 223 K were taken from *DeMore et al.* [1997]. The rate of HCHO photolysis is k_p[HCHO] The chemical reaction rate was calculated as $-d\text{HCHO}/dt = k$ [OH][HCHO], where k is the reaction rate coefficient (1×10^{-11} cm^{-3} $molecule^{-1}$ s^{-1}), and bracketed species indicate concentrations The monthly mean [OH] values from *Spivakovsky et al.* [1990] were scaled to noon conditions by applying a factor of 3 [see *Logan et al*, 1981]. Following the model results presented by *Calvert* [1980], we assumed that at 500 mbar, [HCHO] was 1 order of magnitude lower than surface values (background surface values are 0.3 ppb [*Lowe and Schmidt*, 1983; *Ayers et al.*, 1997]). Owing to the assumptions in their computation the uncertainty in the rates is at least a factor of 3.

Alkanes, alcohols, aldehydes, aliphatic acids, and aromatic hydrocarbons are considered to be the major compounds in this category [*Guenther et al.*, 1995, and references therein]. Estimates of their annual emissions vary by at least a factor of 5 [*Müller*, 1992; *Pacyna and Graedel*, 1995; *Guenther et al.*, 1995], with emission rates in the GEIA (500 Tg C yr^{-1}) at the high end of the previously reported range. Although emissions of these compounds may approach those of isoprene, their yield of HCHO (and H_2) should be much smaller due to the significant loss of intermediate species to aerosols and other surfaces [*Graedel*, 1978]. In the absence of a detailed description of these heterogeneous removal mechanisms, we assume that the loss of reaction intermediates is similar to those of terpene oxidation and that HCHO yields range between 0.1 and 0.3. From (14), with S_i between 100 and 500 Tg C yr^{-1}, we find that the oxidation of these compounds may produce between 0.4 and 12 Tg H_2 yr^{-1}.

The total global H_2 source from the oxidation of nNMHCs estimated here (3 to 24 Tg yr^{-1}) contains considerable uncertainties. Key among these are (1) the yield of HCHO resulting from the complex series of reactions and deposition processes that determine its tropospheric mixing ratios and (2) the relative importances of HCHO destruction by photolysis and by reaction with OH. Note that any reaction scheme used to describe H_2 production from hydrocarbons (Figure 8) must be consistent with that of CO production. The yield of CO from CH_4 oxidation in the reaction sequence used here (~0.95) is within the range of previous estimates (e.g., see the discussion on CO production by *Logan et al.* [1981] and *Tie et al.* [1992]). We can also estimate H_2 production from nNMHCs based upon the reaction scheme presented in Figure 8 and estimates of the annual production rate of CO from nNMHCs. With a CO source (as mass of carbon) of 250 ± 80 Tg C_{CO} yr^{-1} [*World Meteorological Organization (WMO)*, 1995] and an H_2 to C_{CO} reaction mass yield of 0.03 ± 0.01 (determined following the reaction pathways presented in Figure 8), the H_2 production from nNMHCs is 3-15 Tg H_2 yr^{-1}. Similar calculations based upon CO production from the GEIA emission rates would provide H_2 production rates at the high end of this range but still consistent with the H_2 source determined above.

4.1.2. Combustion sources. The combustion of fossil fuels is a major source of atmospheric H_2. *Scranton et al.* [1980] measured H_2 in the Washington, D. C., area and found a diurnal cycle that was well correlated with local traffic patterns, suggesting vehicle use was a major source of H_2 to the urban atmosphere. The global H_2 source from fossil fuel combustion has been estimated as the product of global CO emissions from transportation and the emission ratio of H_2/CO [*Warneck*, 1988]. Aircraft-based measurements of CO and H_2 made within an urban plume near Munich, Germany, indicated an H_2/CO volume ratio of 1 (*Seiler and Zankl* [1975], as referenced by *Conrad and Seiler* [1980]). Our measurements of H_2 and CO made ~30 m above a busy intersection in Boulder, Colorado, during 1989 suggested a mass flux ratio of 0.042 ± 0.007, about half that reported by *Seiler and Zankl* [1975]. The ratio measured in Boulder agrees quite well with similar measurements made in Tsukuba, Japan during 1995 (H_2/CO = 0.035 (Y. Tohjima, Japanese Meteorological Agency, Tsukuba, Japan, personal communication, 1997)). While most estimates of the CO source from transportation fall into a narrow range (200-230 Tg CO yr^{-1} [*Logan et al*, 1981; *Müller*, 1992; *Bradley et al.*, 1999]), the uncertainty of each estimate is large. *Pacnya and Graedel* [1995] suggested an uncertainty for all technological CO sources as ±33%, which we accept as representative of the transportation source. With global production of CO from transportation of 215 ± 70 Tg CO yr^{-1} and vehicle H_2/CO emission ratios of 0.035-0.071, the source of H_2 from transportation is 5-20 Tg yr^{-1}.

Technological processes other than combustion by motor vehicles may also produce H_2; however, as far as we are aware, emissions of H_2 from various industries have not been determined. CO is also emitted from nontransportation-related sources (predominantly heavy industries such as the production of iron and steel and the cracking of crude oil). Rates of CO production from these industries may provide an estimate of the H_2 source. In lieu of measured emissions we estimated H_2/CO mass flux ratios assuming that CO and H_2 mixing ratios in polluted areas result from a mixture of their common urban anthropogenic sources: motor vehicles and technological processes. Average H_2/CO emission ratios for a mixture of urban sources were determined by comparing H_2 and CO mixing ratios in clean and polluted air masses (following *Schmidt* [1974] as described below) and were found to range between 0.004 and 0.03. These ratios represent a mixture of vehicle and industrial emissions, and provide an upper limit on industrial emission ratios. Combined with a CO source strength between 100 and 200 Tg CO yr^{-1} [*Müller*, 1992; *Badr and Probert*, 1994], H_2 production from nonmotor vehicle sources is ~0.4-6 Tg yr^{-1}.

Industrial and technological processes also produce a variety of nonmethane hydrocarbons (primarily alkanes, alkenes, and aromatic compounds). This anthropogenic NMHC source has been estimated to be between 60 and 140 Tg C yr^{-1} [*WMO*, 1995, and references therein]. In the urban atmosphere a diverse mixture of NMHCs react with OH, O_3, and nitrogen oxides to produce numerous reactive products. This diverse mixture of

21562202d, 1999, D23, Downloaded from https://agupubs.onlinelibrary.wiley.com/doi/10.1029/1999JD900788 by INASP/HINARI - PAKISTAN, Wiley Online Library on [07/05/2025]. See the Terms and Conditions (https://onlinelibrary.wiley.com/terms-and-conditions) on Wiley Online Library for rules of use; OA articles are governed by the applicable Creative Commons License

hydrocarbon species may be represented as propylene, and we expect that during the oxidation of these compounds, significant heterogenous loss of reactive intermediates will occur as a result of their low vapor pressures and the high concentrations of particulates found in these environments [*Graedel et al.*, 1976]. Assuming that the HCHO yield from these hydrocarbons is similar to that estimated for terpenes, their H_2 production rate is $\leq$2 Tg H_2 yr^{-1}. The total technology source of H_2, composed predominantly of vehicle emissions, then totals between 6 and 28 Tg yr^{-1}.

As noted above, very few data are available for emissions of H_2 from industrialized processes other than transportation. *Schmidt* [1974] compared measurements of CO and H_2 from a polluted location (Mainz, Germany) to those made in clean air (the North Atlantic). Given that the total flux of two conserved compounds from the same source (or source region) is proportional to the gradients of their concentrations, Schmidt estimated an "anthropogenic" H_2/CO mass flux ratio of ~3%. This ratio represents average H_2/CO emissions for an urban area (including direct emissions from transportation and other industrial processes plus secondary production from the oxidation of anthropogenic hydrocarbons). Following *Schmidt* [1974], we estimated H_2 to CO flux ratios in polluted areas using results from several regionally polluted and marine boundary layer sites at similar latitudes. Monthly mean H_2 and CO mixing ratios were calculated from wintertime data (January-March 1993-1996; i.e., periods when these species should be largely conserved) for the Baltic Sea/Mace Head; Tae-ahn Peninsula/Midway; and North Carolina/Bermuda (see Figure 1 for site locations). The H_2 to CO mass ratios determined from these mixing ratios ranged from 0.4 to 2%, with a mean ratio of 1.3 $\pm$ 0.7%. Using a global source of CO from fossil fuel combustion and other industrial sources of 500 $\pm$ 200 Tg yr^{-1} [*Logan et al.*, 1981; *Pacnya and Graedel*, 1995; *WMO*, 1995] and H_2/CO flux ratios of 0.004 to 0.03, we found the combined H_2 production from all industrial processes ranged from 2 to 21 Tg yr^{-1}. This rate agrees well with that determined as the sum of H_2 emissions from transportation and other technological sources (6-28 Tg yr^{-1}). With a range of emission rates from 2 to 28 Tg H_2 yr^{-1} we estimate that 15 $\pm$ 10 Tg H_2 are emitted by technological processes to the troposphere each year.

The burning of tropical and boreal forests, tropical savannas, agricultural wastes, and wood fuels is a significant source of many trace gases. Previous estimates of the H_2 source from biomass burning range from 5-11 to 21 Tg H_2 yr^{-1} (*Crutzen and Andreae* [1990] and *Laursen et al.* [1992], respectively). Annual H_2 emissions from biomass fires were estimated here based upon the amount of carbon released as CO_2 and H_2/CO_2 emission ratios from a variety of fire types as reported in the literature. Annual average global emissions of CO_2 from biomass burning are between 1.6 and 4.1 $\times$ 10^3 Tg CO_2 yr^{-1} [*Crutzen and Andreae*, 1990]. These emission estimates, when combined with H_2/CO_2 emission ratios ranging from 0.017 to 0.037 [*Crutzen et al.*, 1979; *Crutzen and Andreae*, 1990; *Cofer et al.*, 1989, 1990, 1996], suggest that biomass burning provides between 5 and 27 Tg H_2 to the troposphere each year. The mean production rate derived here (16 Tg H_2 yr^{-1}) falls between the estimates of Crutzen and coworkers and *Laursen et al.* [1992]. The differences between these estimates is largely due to the amount of biomass carbon burned each year as used in the calculations and to differences in emission ratios.

Last, H_2 emissions from the oceans and biological nitrogen fixation provides ~8% of the total source. The individual source strengths of hydrogen sum to 77 $\pm$ 20 Tg H_2 yr^{-1} (Table 2).

4.2. Hydrogen Sinks

4.2.1. Reaction with OH. Hydrogen is removed from the atmosphere primarily through soil uptake and by reaction with OH (reaction (1)). The loss rate of H_2 due to oxidation by OH (L_{OH}) is proportional to the abundances of H_2 and OH:

$$L_{OH} = - k_1[OH](G_{H2}), \quad (15)$$

where k_1 is the reaction rate constant of H_2 + OH at 277 K, (4.0 $\pm$ 0.2) $\times$ 10^{-15} cm^3 $molecule^{-1}$ s^{-1}; [OH] = (9.7 $\pm$ 0.6) $\times$ 10^5 molecules cm^{-3}; and G_{H2} is the global annual average tropospheric H_2 burden. G_{H2} during the period 1991-1996 (155 $\pm$ 10 Tg) was determined using a average tropospheric H_2 mixing ratio of 531 $\pm$ 6 ppb and assuming no H_2 gradient with altitude (see *Schmidt* [1974] and *Ehhalt et al.* [1977]; also compare the time series from Cape Kumukahi (3 m asl) and Mauna Loa (3347 m asl), Hawaii, in Figure 3). From (15) we find OH removes between 16 and 22 Tg H_2 yr^{-1}. The difference between this photochemical H_2 loss rate and our mean annual source (~80 Tg yr^{-1}) implies a surface uptake rate of ~60 Tg yr^{-1}.

4.2.2. Soil uptake. The surface deposition rate of H_2 is the largest term in the global budget and is also one of the most poorly defined. Loss of tropospheric H_2 to the Earth's surface (L_{soil}) has been estimated from surface deposition velocities and the tropospheric concentration of H_2:

$$L_{soil} = -v_d n[H_2]A_e \quad (16)$$

where v_d is the global average deposition velocity for hydrogen; n is the average surface number density (2.7 $\times$ 10^{19} molecules cm^{-3}); [H_2] is annual average H_2 mixing ratio (531 ppb); and A_e is effective Earth soil surface area (90 $\times$ 10^6 km^2 [*Conrad and Seiler*, 1980]). Deposition rates are sensitive to soil conditions such as temperature [*Liebl and Seiler*, 1976; *Hurst et al.*, 1996] and moisture [*Conrad and Seiler*, 1980; 1985], and the range of v_d measured by Seiler and coworkers (< 1 $\times$ 10^{-2} to 1.4 $\times$ 10^{-1} cm s^{-1}) probably reflects diverse soil conditions. *Conrad and Seiler* [1980; 1985] represented global conditions using v_d = 7 $\times$ 10^{-2} cm s^{-1} and calculated a global surface H_2 deposition rate of 70 to 110 Tg H_2 yr^{-1}. *Schmidt et al.* [1980] estimated global H_2 uptake by various ecosystems, and from their analysis a global average deposition velocity of 0.035 cm s^{-1} can be derived. Measurements of landscape-scale (several square kilometers) atmosphere-soil fluxes of H_2 made from a 400-m tower in Wisconsin indicated an annual average deposition velocity to predominantly wet soils of ~1 $\times$ 10^{-2} cm s^{-1} [*Hurst et al.*, 1996]. Here we use deposition velocities between 1 and 7 $\times$ 10^{-2} cm s^{-1} to represent annually averaged global values, and the soil sink determined from (16) is then between 15 and 96 Tg H_2 yr^{-1}. This estimate is similar to that determined by *Schmidt et al.* [1980] (20-107 Tg yr^{-1}) but somewhat lower than the estimates of Conrad and Seiler (e.g., 70-110 Tg H_2 yr^{-1} [*Conrad and Seiler*, 1980, 1985]. The sum of L_{OH} and L_{soil} determined in this study gives a total sink of 75 $\pm$ 41 Tg H_2 yr^{-1}.

The mean global H_2 source and sink strengths estimated here (77 and 75 Tg yr^{-1}, respectively) are slightly lower than previous estimates, although the uncertainties are considerable (Table 2). We attribute ~25% of the global sink to reaction with OH, in good agreement with *Schmidt et al.* [1980] but 2-3 times the estimates of *Conrad and Seiler* [1980, 1985] and *Warneck*

21562202d, 1999, D23, Downloaded from https://agupubs.onlinelibrary.wiley.com/doi/10.1029/1999JD900788 by INASP/HINARI - PAKISTAN, Wiley Online Library on [07/05/2025]. See the Terms and Conditions (https://onlinelibrary.wiley.com/terms-and-conditions) on Wiley Online Library for rules of use; OA articles are governed by the applicable Creative Commons License

[1988] (8 to 12%). The difference between these estimates is due to both the value of [OH] used; in this work [OH] = 9.7×10^5 molecules cm^{-3} s^{-1}, about twice that used by *Conrad and Seiler* [1980] and *Warneck* [1988], and due to the range of deposition velocities used to estimate soil uptake. We find that with total source and sink strengths of the order of 50-90 Tg yr^{-1} and a tropospheric burden of 155 Tg the globally averaged lifetime of H_2 in the troposphere is ~2 to 3 years.

In addition, we note that the relative importances of the soil sink and loss by reaction with OH reported above are inconsistent with those suggested by deuterium/hydrogen (D/H) ratios in air [*Ehhalt and Volz,* 1976]. These data, combined with the ratio of the reaction rate of H_2 + OH to that of HD + OH (the isotopic fractionation factor), suggest that loss of H_2 by reaction with OH could be of similar magnitude as H_2 loss to soils [*Ehhalt et al.*, 1989]. This implies that we have either significantly underestimated the photochemical loss rate of H_2 or, more likely, that the best value for a globally averaged deposition velocity lies at the low end of the range used here ($1\text{-}7 \times 10^{-1}$ cm s^{-1}). If soil and photochemical sinks have similar magnitude, the total H_2 source would lie at the low end of the estimated range.

While significant uncertainties remain in the global H_2 budget, it is nevertheless useful to examine the hemispheric partitioning of the major H_2 sources and sinks. The hemispheric partitioning of H_2 production should follow that of carbon monoxide because both species have common anthropogenic and natural sources [*Logan et al.*, 1981]. Using the hemispheric distribution of CO sources provided by *Logan et al.* [1981] and *Wang et al.* [1998], we expect that ~65% of the global H_2 source is in the NH. The combination of hemispheric H_2 production rates (based upon the distribution of CO sources) with the loss rate due to H_2 + OH allows a mass balance approach to estimate the distribution of the remaining sink strength between the two hemispheres:

$$(dG/dt)_{NH} = k_T [G_N - G_S] + P_{NH} - 0.5L_{OH} - S_{NH}$$

$$(dG/dt)_{SH} = k_T [G_N - G_S] + P_{SH} - 0.5L_{OH} - S_{SH}, \quad (17)$$

where dG/dt is the rate of change in the tropospheric H_2 burden and the subscripts NH and SH indicate the Northern and Southern Hemisphere (dG/dt = -0.4 Tg yr^{-1} in the NH and 0.3 Tg yr^{-1} in the SH; these rates were determined from time series displayed in Figure 6); k_T is the interhemispheric exchange coefficient (0.97 yr^{-1}) [*Warneck,* 1988]; G_N and G_S are the NH and SH H_2 burdens (76.3 and 78.6 Tg, respectively), and P is the hemispheric production rate (derived from the hemispheric distribution of CO sources): 49 and 27 Tg yr^{-1} in the NH and SH, respectively. L_{OH} is the photochemical destruction rate of H_2 determined above (section 4.2.1, L_{OH} = 20 Tg yr^{-1})]. We assume that L_{OH} is equal in both hemispheres (while OH may be slightly lower in the SH compared to the NH (1000-500 mbar; from *Spivakovsky et al.* [1990]), greater H_2 in the SH nearly balances the reaction rate). S, the undefined sink, is then ~38 Tg yr^{-1} in the NH and ~16 Tg yr^{-1} in the SH. Given that the only major sink identified for H_2 other than photochemical loss is surface deposition, and we estimate that ~60-70% of the vegetated land area is in the NH, the hemispheric difference in mixing ratios may be reasonably attributed to the effectiveness of soil uptake (as first suggested by *Khalil and Rasmussen* [1990]).

The seasonal cycle of H_2 reflects both the locations and seasonal variations of its sources and sinks and was found to vary with latitude (Figures 3 and 6). In the NH we expect that the maximums observed in late winter were largely driven by the absence of a strong sink combined with seasonally independent technological emissions and a maximum in tropical biomass burning. The early fall minimums were driven by a combination high levels of OH (and high rates of photochemical H_2 loss) and strong soil uptake. In the LSH the observed springtime maximums corresponded in timing to the typical period of greatest biomass burning (September and October [*Delas et al.*, 1991]), a time when rates of H_2 production from CH_4 and nNMHCs are also near their maximum. These sources, particularly a pulse of H_2 from biomass burning, may overwhelm peak summertime removal by soils and OH. Maximum H_2 mixing ratios in the HSH occurred 3-4 months after the maximum in the southern tropics (Figure 6), an offset consistent with poleward transport of H_2 from a strong tropical source such as biomass burning.

5. Summary and Conclusions

Measurements of H_2 in the remote marine boundary layer were made at ~50 locations during the past 5 years. These show that H_2 mixing ratios were typically lower in the NH than in the SH. The greatest abundance of H_2 was observed in the southern tropics. The H_2 seasonal cycle was well defined, with maximum levels in the NH occurring in late winter/early spring and minimum levels in fall. In the SH the seasonal minimum occurred in late winter/spring and the maximum occurred in late spring/early summer. The seasonal maximum in the SH may be largely driven by tropical biomass burning. The amplitude of the seasonal cycle in the HNH was about 3 times that in the LSH, due in part to differences in the strength of the seasonal drawdown among the two hemispheres. We suggest this is due to greater soil uptake in the NH compared with that in the SH.

Trends in the zonally averaged H_2 time series (section 3, Figure 6) were estimated using (2) with $a_3 = 0$. During 1991-1996, the globally averaged H_2 mixing ratio in the MBL decreased at an apparent rate of 2.3 ± 0.1 ppb yr^{-1} (= 0.44% yr^{-1}). The trend is largely due to high H_2 mixing ratios in late 1991 through early 1992 (enhancements of 8-12 ppb were observed at Ascension Island, Christmas Island, Cape Kumukahi, Mauna Loa, and Samoa), followed by a sharp decline during 1992-1993. The average rate of change in the NH (-2.7 ± 0.2 ppb yr^{-1}) was slightly greater than in the SH (2.0 ± 0.2 ppb yr^{-1}). During the period of this study, tropospheric CO also decreased [*Khalil and Rasmussen*, 1994; *Novelli et al.*, 1994, 1998; *Mathieu et al.*, 1997]. The relationship between CO and H_2 provides insight to possible causes of the recent changes in both species. Combustion of fossil fuels and biomass are major sources for both gases, and a decline in emissions from either would decrease their tropospheric abundances. The observed decrease in CO is consistent with declines in NH emissions from motor vehicles [*Bakwin et al.*, 1994; *Granier et al.*, 1996], combined with diminished production from the burning of biomass [*Novelli et al.*, 1994; *Granier et al.*, 1996]. Changes in these combustion sources would also tend to suppress tropospheric H_2. Changes in OH due to the eruption of Mount Pinatubo in June 1991 may have contributed to interannual variations in both CO [i.e., *Bekki et al.*, 1994; *Dlugokencky et al.*, 1996] and H_2 mixing ratios but only slightly to their apparent decreasing trends [*Novelli et al.*, 1994].

In contrast to the results reported here, measurements of H_2 at Cape Grim, Tasmania, by the Commonwealth Scientific and Industrial Organization (CSIRO), Division of Atmospheric

21562202d, 1999, D23, Downloaded from https://agupubs.onlinelibrary.wiley.com/doi/10.1029/1999JD900788 by INASP/HINARI - PAKISTAN, Wiley Online Library on [07/05/2025]. See the Terms and Conditions (https://onlinelibrary.wiley.com/terms-and-conditions) on Wiley Online Library for rules of use; OA articles are governed by the applicable Creative Commons License

Research, Aspendale, Victoria, Australia, show a slight increase in H_2 from 1992 to 1997 (P. Steele, personal communication, 1999). An ongoing intercomparison of trace gas measurements between NOAA/CMDL and CSIRO show a widening divergence in measured H_2 mixing ratios (≈2.3 ppb yr^{-1} (K. A. Masarie et al., manuscript in preparation, 1999)). While the reason(s) for the difference between labs is not yet known, it is not believed to be related to the sampling protocols. Instead, it may be due to undetected drift in standard gases, or other differences related to the measurement calibration (such as instrument deviation from linear response).

Considerable uncertainties remain in the the global budget of H_2. Nevertheless, we find that the oxidation of CH_4 is the largest source of H_2 to the atmosphere (30%), with production from the oxidation of natural NMHCs, technological processes, and biomass burning each ~20% of the global source. Surface deposition accounts for about 75% of the tropospheric sink, with the remainder due to reaction with OH. Total sources are balanced, within error, by total sinks. With an annual turnover of ~75 Tg yr^{-1} and an average tropospheric burden of 155 Tg, the lifetime of H_2 is about 2 years.

Last, we note that the error associated with any particular term in the H_2 budget is between ±30% and ±60%. Measurements of the isotopic ratios of deuterium (D) to hydrogen (H) in atmospheric H_2 could improve our understanding of the H_2 budget. Strong mass-dependent fractionation of D to H by the reaction of H_2 + OH, and fractionation during H_2 production by photochemical and combustion processes, contrasts the relatively weak fractionation by soil uptake [*Ehhalt and Volz*, 1976]. Differences in the isotopic signatures of the major sources and sinks may provide a means of deconvoluting the complex signals of the biogeochemical cycle of hydrogen. Unfortunately, the isotopic fractionation associated with these processes still contain large uncertainties [*Ehhalt and Volz*, 1976; *Ehhalt et al.*, 1989; D. Ehhalt, personal communication, 1997]. More measurements of D/H in atmospheric H_2, combined with additional information on the fractionation of D/H during the various processes of H_2 production and destruction, could help constrain the uncertainties in the global budget.

Acknowledgments. Participants in the cooperative air sampling network are acknowledged for collecting the air samples. The Blue Star, Chevron, and Nippon shipping lines provided samples from the Pacific Ocean. C. Proskto-Bell and L. S. Waterman managed the sampling network, and K. W. Thoning developed many of the smoothing algorithms used here. E. J. Dlugokencky and P. P. Tans both provided valuable discussions which added to this paper. Three anonymous reviewers made many helpful comments on the manuscript. The air sampling network and CO/H_2 measurements were supported by the Radiatively Important Trace Gas Species and Atmospheric Chemistry components of the NOAA Climate and Global Change Program. The calibration system was supported in part by the World Meteorological Organization

References

Ayers, G.P., R.W. Gillet, and H. Granek, Formaldehyde production in clean marine air, *Geophys. Res. Lett., 24*, 401-404, 1997.

Badr, O., and S.D. Probert, Sources of atmospheric carbon monoxide, *Appl. Energy, 49*, 145-195, 1994.

Bakwin, P.S., P.P. Tans, and P.C. Novelli, Carbon monoxide budget in the northern hemisphere, *Geophys. Res. Lett., 21*, 433-436, 1994.

Bekki, S., K.S. Law, and J.A. Pyle, Effect of ozone depletion on atmospheric CH_4 and CO concentrations, *Nature, 371*, 595-597, 1994.

Bradley, K.S., D.H. Stedman, G.A. Bishop, Global inventory of carbon monoxide emissions from motor vehicles, *Chemosphere*, in press, 1999.

Brasseur, G.P., D.A. Hauglustaine, S. Walters, P.J. Rasch, J.-F. Müller, C. Granier, and X.X. Tie, MOZART, A global chemical transport model for ozone and related chemical tracers, 1, Model description, *J. Geophys. Res., 103*, 28,265-28,289, 1998.

Calvert, J.G., The homogeneous chemistry of formaldehyde generation and destruction with the atmosphere, in *Proceedings of the NATO Advanced Study Institute on Atmospheric Ozone: Its Variation and Human Influences*, edited by A.C. Aikin, and M. Nicholet, *Rep. FAA-EE-80-20*, pp. 153-190, U.S. Dep. of Transp., Washington, D. C., 1980.

Cofer, W.R. III, J.S. Levine, D.I. Sebacher, E.L. Winstead, P.J. Riggin, B.J. Stocks, J.A. Brass, V.G. Ambrosia, and P.J. Boston, Trace gas emissions from chaparral and boreal forest fires, *J. Geophys. Res., 94*, 2255-2259, 1989.

Cofer, W.R. III, J.S. Levine, E.L. Winstead, P.J. LeBel, A.M. Koller Jr., and R. Hinkle, Trace gas emissions from burning Florida wetlands, *J. Geophys. Res., 95*, 1865-1870, 1990.

Cofer, W.R. III, J.S. Levine, E.L. Winstead, D.R. Cahoon, D.I. Sebacher, J.P. Pinto, and B.J. Stocks, Source compositions of trace gases released during African savanna fires, *J. Geophys. Res., 101*, 23,597-23,602, 1996.

Cohan, D.S., M.G. Schultz, D.J. Jacob, B.G. Heikes, and D.R. Blake, Convective injection and photochemical decay of peroxides in the upper tropical troposphere: Methyl iodide as a tracer of marine convection, *J. Geophys. Res., 104*, 5717-5724, 1999.

Conrad, R., and W. Seiler, Contribution of hydrogen production by biological nitrogen fixation to the global hydrogen budget, *J. Geophys. Res., 85*, 5493-5498, 1980.

Conrad, R., and W. Seiler, Influence of temperature, moisture, and organic carbon on the flux of H_2 and CO between soil and atmosphere: Field studies in subtropical regions, *J. Geophys. Res., 90*, 5699-5709, 1985.

Conway, T.J., P.P. Tans, L.S. Waterman, K.W. Thoning, D.R. Kitzis, K.A. Masarie, and N. Zhang, Evidence for the interannual variability of the carbon cycle from the National Oceanic and Atmospheric Administration Climate Monitoring and Diagnostics Laboratory global air sampling network, *J. Geophys. Res., 99*, 22,831-22,855, 1994.

Crutzen, P.J., Methane's sinks and sources, *Nature, 350*, 380-381, 1991.

Crutzen, P.J , and M.O. Andreae, Biomass burning in the tropics: Impact on atmospheric chemistry and biogeochemical cycles, *Science, 250*, 1669-1678, 1990.

Crutzen, P.J., L.E. Heidt, J.P. Krasnec, W.H. Pollack, and W. Seiler, Biomass burning as a source of atmospheric gases CO, H_2, N_2O, NO, CH_3Cl, and COS, *Nature, 282*, 253-256, 1979.

Delas, R.A., P. Loudjani, A. Podaire, and J.-C. Menaut, Biomass burning in Africa: An assessment of annually burned biomass, in *Global Biomass Burning: Atmospheric, Climatic, and Biospheric Implications*, edited by J.S. Levine, pp. 126-132, MIT Press, Cambridge, Mass., 1991.

Demerjian, K.L., K.L. Schere, and J.T. Peterson, Theoretical estimates of actinic (spherically integrated) flux and photolytic rate constants of atmospheric species in the lower troposphere, *Adv. Environ. Sci. Technol., 10*, 369-412, 1980.

DeMore, W B., S.P. Sander, D.M. Golden, R.F. Hampson, K.J. Kurylo, C.J. Howard, A.R Ravishankara, and M.J. Molina, *Chemical Kinetics and Photochemical Data for Use in Stratospheric Modeling, Evaluation 12, JPL Publ. 97-4*, 266 pp., 1997.

de Serves, C , Gas phase formaldehyde and peroxide measurements in the Arctic atmosphere, *J. Geophys. Res., 99*, 25,391-25,398, 1994.

Dlugokencky, E.J., L.P. Steele, P.M. Lang, and K.A. Masarie, The growth rate and distribution of atmospheric methane, *J. Geophys. Res., 99*, 17,021-17,043, 1994.

Dlugokencky, E.J., E.G. Dutton, P.C. Novelli, P.P. Tans, K.A. Masarie, K.O. Lantz, and S. Madronich, Changes in CH_4 and CO growth rates after the eruption of Mt. Pinatubo and their link with changes in tropical UV flux, *Geophys. Res. Lett., 23*, 2761-2764, 1996.

Ehhalt, D.H., and A. Volz, Coupling of the CH_4 with the H_2 and CO cycle: Isotopic evidence, in *Production and Utilization of Gases*, edited by H.G. Schlegel, G. Gottschalk, and N. Pfennig, pp. 23-33, E. Golze, Göttingen, Germany, 1976.

Ehhalt, D.H., U. Schmidt, and L.E. Heidt, Vertical profiles of molecular hydrogen in the troposphere and stratosphere, *J. Geophys. Res., 82*, 5907-5911, 1977.

21562202d, 1999, D23, Downloaded from https://agupubs.onlinelibrary.wiley.com/doi/10.1029/1999JD900788 by INASP/HINARI - PAKISTAN, Wiley Online Library on [07/05/2025]. See the Terms and Conditions (https://onlinelibrary.wiley.com/terms-and-conditions) on Wiley Online Library for rules of use; OA articles are governed by the applicable Creative Commons License

Ehhalt, D.H., J.A. Davidson, C.A. Cantrell, I. Friedman, and S. Tyler, The kinetic isotope effect in the reaction of H_2 with OH, *J. Geophys. Res., 94*, 9831-9836, 1989.

Fehsenfeld, F., et al., Emissions of volatile organic compounds from vegetation and the implications for atmospheric chemistry, *Global Biogeochem. Cycles, 6*, 389-430, 1992.

Finlayson-Pitts, B.J., and J.N. Pitts Jr., *Atmospheric Chemistry: Fundamentals and Experimental Techniques*, 1098 pp., John Wiley, New York, 1986.

Graedel, T.E., *Chemical Compounds in the Atmosphere*, Academic, San Diego, Calif., 440 pp., 1978.

Graedel, T.E., Terpenoids in the troposphere, *Rev. Geophys., 17*, 937-947, 1979.

Graedel, T.E., and P.J. Crutzen, *Atmospheric Change: An Earth System Perspective*, 446 pp., W.H. Freeman, New York, 1993.

Graedel, T.E., L.A. Farrow, and T.A. Weber, Kinetic studies of the photochemistry of the urban troposphere, *Atmos. Environ., 10*, 1095-1116, 1976.

Granier, C., J.-F. Müller, S. Madronich, and G.P. Brasseur, Possible causes of the 1990-1993 decrease in the global tropospheric carbon monoxide abundance: A three dimensional sensitivity study, *Atmos. Environ., 30*, 1673-1682, 1996.

Grenier, N.P., Hydroxyl radical kinetics by kinetic spectroscopy, V, Reactions with H_2 and CO in the range 300-500°K, *J. Chem. Phys., 51*, 5049-5051, 1969.

Guenther, A., et al., A global model of natural volatile organic compound emissions, *J. Geophys. Res., 100*, 8873-8892, 1995.

Hatakeyama, S., K. Izumi, T. Fukuyama, H. Akimoto, and N. Washida, Reactions of OH with α-pinene and β-pinene in air: Estimates of CO production from the oxidation of terpenes, *J. Geophys. Res., 96*, 947-958, 1991.

Hurst, D.F., P.S. Bakwin, C. Zhoa, K.J. Davis, and R.M. Teclaw, Landscape-scale surface fluxes of methane and hydrogen in a North American boreal lowland and wetland boreal forest, *Eos Trans. AGU, 77*(46), Fall Meet. Suppl., F124-F125, 1996.

Intergovernmental Panel on Climate Change (IPCC), *Climate Change 1995*, 572 pp., Cambridge Univ. Press, New York, 1996.

Jacob, D.J., and S.C. Wofsy, Photochemistry of biogenic emissions over the Amazon forest, *J. Geophys. Res., 93*, 1477-1486, 1988.

Jacob, D.J., and S.C. Wofsy, Budgets of reactive nitrogen, hydrocarbons, and ozone over the Amazon forest during the wet season, *J. Geophys. Res., 95*, 16,737-16,754, 1990.

Khalil, M.A.K., and R.A. Rasmussen, Distribution and mass balance of molecular hydrogen in the Earth's atmosphere, in *Geophysical Monitoring for Climatic Change, No. 17, Summary Report 1988*, edited by J.W. Elkins and R.R. Rosson, pp. 111-113, NOAA Air Resour., Lab., Boulder, Colo., 1989.

Khalil, M.A.K., and R.A. Rasmussen, Global increase of atmospheric molecular hydrogen, *Nature, 347*, 743-745, 1990.

Khalil, M.A.K., and R.A. Rasmussen, Global decrease in atmospheric carbon monoxide, *Nature, 370*, 639-641, 1994.

Laursen, K.K., P.V. Hobbs, L.F. Radke, and R.A. Rasmussen, Some trace gas emissions from North American biomass fires with an assessment of regional and global fluxes from biomass burning, *J. Geophys. Res., 97*, 20,681-20,701, 1992.

Liebl, K.H., and W. Seiler, CO and H_2 destruction at the soil surface, in *Production and Utilization of Gases*, edited by H.G. Schlegel, G. Gottschalk, and N. Pfennig, pp. 215-229, E. Golze, Göttingen, Germany, 1976.

Logan, J.A., M.J. Prather, S.C. Wofsy, and M.B. McElroy, Tropospheric chemistry: A global perspective, *J. Geophys. Res., 86*, 7210-7252, 1981.

Lowe, D.C., and U. Schmidt, Formaldehyde (HCHO) measurements in the nonurban atmosphere, *J. Geophys. Res., 88*, 10,844-10,585, 1983.

Mathieu, E., R. Zander, L. Delbouille, P. Demoulin, G. Roland, and C Servais, Observed trends in total vertical column abundances of atmospheric gases from IR spectra recorded at the Jungfrauhoch, *J. Atmos. Chem., 28*, 227-243, 1997.

Moortgat, G.K., and P. Warneck, Photodecomposition of formaldehyde, *J. Chem. Phys., 70*, 3639-3651, 1979.

Moortgat, G.K., W. Seiler, and P. Warneck, Photodissociation of CH_2O in air: CO and H_2 quantum yields at 220 and 300 K, *J. Chem. Phys., 78*, 1185-1190, 1983.

Müller, J.-F., Geographical distribution and seasonal variation of surface emissions and deposition velocities of atmospheric trace gases, *J. Geophys. Res., 97*, 3787-3804, 1992.

Müller, J.-F., and G. Brasseur, IMAGES: A three-dimensional chemical transport model of the global troposphere, *J. Geophys. Res., 100*, 16,445-16,490, 1995.

Novelli, P.C., J.W. Elkins, and L.P. Steele, The development and evaluation of a gravimetric reference scale for measurements of atmospheric carbon monoxide, *J. Geophys. Res., 96*, 13,109-13,121, 1991.

Novelli, P.C., L.P. Steele, and P.P. Tans, Mixing ratios of carbon monoxide in the troposphere, *J.Geophys. Res., 97*, 20,731-20,750, 1992.

Novelli, P.C., K.A. Masarie, P.P. Tans, and P.M. Lang, Recent changes in atmospheric carbon monoxide, *Science, 263*, 1587-1590, 1994.

Novelli, P.C., K.A. Masarie, and P.M. Lang, Distributions and recent trends of carbon monoxide in the lower troposphere, *J. Geophys. Res., 103*, 19,015-19,033, 1998.

Pacyna, J.M., and T.E. Graedel, Atmospheric emissions inventories: Status and prospects, *Annu. Rev. Energy Environ., 20*, 265-300, 1995.

Paulson, S.E. and J.H. Seinfeld, Development and evaluation of a photochemical mechanism for isoprene, *J. Geophys. Res., 97*, 20,703-20,715, 1992.

Prinn, R.G., R.F. Weiss, B.R. Miller, J. Huang, F.N. Alyea, D.M. Cunnold, P.J. Fraser, D.E. Hartley, and P.G. Simmonds, Atmospheric trends and lifetime of CH_3CCl_3 and global OH concentrations, *Science, 269*, 187-192, 1995.

Ravishankara, A.R., Kinetics of radical reactions in the atmospheric oxidation of CH_4, *Annu. Rev. Phys. Chem., 39*, 367-394, 1988.

Schmidt, U., Molecular hydrogen in the atmosphere, *Tellus, 56*, 78-90, 1974.

Schmidt, U., and W. Seiler, A new method for recording molecular hydrogen in atmospheric air, *J. Geophys. Res., 75*, 1713-1716, 1970.

Schmidt, U., G. Kulessa, and E.P. Roth, The atmospheric H_2 cycle, in *Proceedings of the NATO Advanced Study Institute on Atmospheric Ozone: Its Variation and Human Influences*, edited by A.C. Aikin, and M. Nicholet, *Rep. FAA-EE-80-20*, pp. 307-322, U.S. Dep. of Transp. Washington, D. C., 1980.

Scranton, M.I., W.R. Barger, and F.L. Herr, Molecular hydrogen in the urban troposphere: Measurement of seasonal variability, *J. Geophys. Res., 85*, 5575-5580, 1980.

Seiler, W., and R. Conrad, Contribution of tropical ecosystems to the global budgets of trace gases, especially CH_4, H_2, CO, and N_2O, in *The Geophysiology of Amazonia: Vegetation and Climate Interactions*, edited by R.E. Dickerson, pp. 33-62, John Wiley, New York, 1987.

Seiler, W., and H. Zankl, Die Spurengase CO und H_2 uber Munchen, *Umschau, 75*, 735-736, 1975.

Snedecor, G.W., and W.G. Cochran, *Statistical Methods*, 6th ed., 593 pp., Iowa State Univ. Press, Ames, 1967.

Solberg, S., C. Dye, N. Schmidbauer, A. Herzog, and R. Gehrig, Carbonyls and nonmethane hydrocarbons at rural European sites from the Mediterranean to the Arctic, *J. Atmos. Chem.*, 25, 33-66, 1996.

Spivakovsky, C.M., R. Yevich, J.A. Logan, S.C. Wofsy, and M.B. McElroy, Tropospheric OH in a three-dimensional chemical tracer model: An assessment based on observations of CH_3CCl_3, *J. Geophys. Res., 95*, 18,441-18,471, 1990.

Steele, L.P., E.J. Dlugokencky, P.M. Lang, P.P. Tans, R.C. Martin, and K.A. Masarie, Slowing down of the global accumulation of atmospheric methane during the 1980s, *Nature, 358*, 313-316, 1992.

Stockwell, W.R., and J.G. Calvert, The mechanism of NO_3 and HONO formation in the nighttime chemistry of the urban atmosphere, *J. Geophys. Res., 88*, 6673-6682, 1983.

Tans, P.P., T.J. Conway, and T. Nakazawa, Latitudinal distributions of the surface sources and sinks of atmospheric CO_2 derived from surface observations and an atmospheric transport model, *J. Geophys. Res., 94*, 5151-5172, 1989.

Taylor, J.A., P. Zimmerman, and D. Erickson, A 3-D modelling study of the sources and sinks of atmospheric carbon monoxide, paper presented at *CRES Workshop*, Aust. Nat. Univ., Canberra, 1990.

Thoning, K.W., P.P. Tans, and W.D. Komhyr, Atmospheric carbon dioxide at Mauna Loa Observatory, 2, Analysis of the NOAA GMCC data, 1974-1985, *J. Geophys. Res., 94*, 8549-8576, 1989.

Tie, X.X., C.-Y. J. Kao, and E.J. Mroz, Net yield of OH, CO, and O_3 from the oxidation of atmospheric methane, *Atmos. Environ, Part A, 26*, 125-136, 1992.

21562202d, 1999, D23, Downloaded from https://agupubs.onlinelibrary.wiley.com/doi/10.1029/1999JD900788 by INASP/HINARI - PAKISTAN, Wiley Online Library on [07/05/2025]. See the Terms and Conditions (https://onlinelibrary.wiley.com/terms-and-conditions) on Wiley Online Library for rules of use; OA articles are governed by the applicable Creative Commons License

Wang, Y., D.J. Jacob, and J.A. Logan, Global simulation of tropospheric O_3-NO_x-hydrocarbon chemistry, 1, Model formulation, *J Geophys. Res., 103*, 10,713-10,725, 1998.

Warneck, P., *Chemistry of the Natural Atmosphere*, *Int. Geophys. Ser.*, vol. 41, 757 pp., Academic, San Diego, Calif., 1988.

Warneck, P., W. Kippel, and G.K. Moortgat, Formaldehyd in troposph ärischer Reinluft, Ber. Bunsenges, *Phys. Chem., 82*, 1136-1142,1978.

World Meteorological Organization (WMO), Scientific Assessment of Ozone Depletion: 1994, *Rep. 37*, Global Ozone Res. and Monit. Proj., Geneva, Switzerland, 1995.

Zafiriou, O.C., J. Alford, M. Herrera, E.T. Peltzer, R.B. Gagosian, and S.C. Liu, Formaldehyde in remote marine air: Flux measurements and estimates, *Geophys. Res. Lett., 7*, 341-344, 1980.

Zimmerman, P.R., R.B. Chatfield, J. Fishman, P. Crutzen, and P.L. Hanst., Estimates on the production of CO and H_2 from the oxidation of hydrocarbon emissions from vegetation, *Geophys. Res. Lett.*, 5, 679-682, 1978.

J. W. Elkins, D. F. Hurst, P. M. Lang, K. A. Masarie, and P. C. Novelli, NOAA/CMDL, 325 Broadway, R/E/CG1, Boulder, CO 80303. (pnovelli@cmdl.noaa.gov)

R. Myers, Standards and Certification Center, NIST, GMCM, 8393, 100 Bureau Drive, Gaithersburg, MD 20899.

(Received March 24, 1999; revised July 20, 1999;
accepted July 26, 1999.)

21562202d, 1999, D23, Downloaded from https://agupubs.onlinelibrary.wiley.com/doi/10.1029/1999JD900788 by INASP/HINARI - PAKISTAN, Wiley Online Library on [07/05/2025]. See the Terms and Conditions (https://onlinelibrary.wiley.com/terms-and-conditions) on Wiley Online Library for rules of use; OA articles are governed by the applicable Creative Commons License